Published in final edited form as:
Cell Motil Cytoskeleton. 2009 August ; 66(8): 567–587. doi:10.1002/cm.20367.

The Effects of Extracellular Calcium on Motility, Pseudopod and Uropod Formation, Chemotaxis and the Cortical Localization of Myosin II in *Dictyostelium discoideum*

Daniel F. Lusche, **Deborah Wessels**, and **David R. Soll**
The W.M. Keck Dynamic Image Analysis Facility, Department of Biology, The University of Iowa, Iowa City, IA 52242

Abstract

Extracellular Ca^{++}, a ubiquitous cation in the soluble environment of cells both free living and within the human body, regulates most aspects of amoeboid cell motility, including shape, uropod formation, pseudopod formation, velocity and turning in *Dictyostelium discoideum*. Hence it affects the efficiency of both basic motile behavior and chemotaxis. Extracellular Ca^{++} is optimal at 10 mM. A gradient of the chemoattractant cAMP generated in the absence of added Ca^{++} only affects turning, but in combination with extracellular Ca^{++}, enhances the effects of extracellular Ca^{++}. Potassium, at 40 mM, can substitute for Ca^{++}. Mg^{++}, Mn^{++}, Zn^{++} and Na^{+} cannot. Extracellular Ca^{++}, or K^{+}, also induce the cortical localization of myosin II in a polar fashion. The effects of Ca^{++}, K^{+} or a cAMP gradient do not appear to be similarly mediated by an increase in the general pool of free cytosolic Ca^{++}. These results suggest a model, in which each agent functioning through different signaling systems, converge to affect the cortical localization of myosin II, which in turn effects the behavioral changes leading to efficient cell motility and chemotaxis.

Keywords

Calcium; potassium; cAMP; cell motility; chemotaxis

Introduction

Ca^{++} is the fifth most abundant element in the earth's lithosphere (Day, 1963), the fourth most abundant element in igneous and sedimentary rocks, usually the most abundant cation in freshwater and the third most abundant cation in seawater (Hem, 1970, 1989). In the aqueous environment, the concentration of free Ca^{++} varies dramatically between oceans, rivers, lakes and soil-solutions (Goldberg *et al.*, 1971; Dodds, 2002; Dauer, *et al.*, 2007; Bangerth, 1979; McLaughlin and Wimmer, 1999). It can also vary within a body of water over time through precipitation, evaporation, the melting of ice and exchange with catchment soil (Jeziorski *et al.*, 2008). In soil solutions, the concentration of free Ca^{++} standardly varies between 3.4 and 14 mM (Bangerth, 1979; McLaughlin and Wimmer, 1999), but can undergo even greater transient fluctuations due to precipitation and evaporation. Hence, organisms like the soil amoeba *Dictyostelium discoideum*, which depend upon amoeboid motility in one or more phases of their life histories, can experience dramatic changes in the Ca^{++} concentration of the environment in which they migrate.

Please direct all correspondence to: David R. Soll, 302 BBE, Department of Biology, The University of Iowa, Iowa City, IA 52242, Tel: (319) 335-1117, Fax: (319) 335-2772, david-soll@uiowa.edu.

In the human body, the concentration of free Ca^{++} also varies between tissues and fluids. For instance, in serum the concentration is between 2.2 and 2.6 mM (Silver *et al.*, 1988), and in the extracellular fluids of tissues, it can vary between 1.1 and 1.3 mM (Breitwieser, 2008). At erosion sites of osteoporotic fragments (Silver *et al.*, 1988; Breitwieser, 2008), free Ca^{++} can reach concentrations as high as 20 to 40 mM. Ca^{++} also forms spatial gradients emanating from sites of Ca^{++} deposition and erosion, which attract stromal cells and osteoblasts (Godwin and Soltoff, 1997; Yamaguchi *et al.*, 1998; Sugimoto *et al.*, 1993), and has been shown to play a role in the migration of axons (Zheng and Poo, 2007), smooth muscle cells (Scherberich *et al.*, 2000) and white blood cells (Randolph *et al.*, 2008; Clark and Petty, 2008; Kindzelskii *et la.*, 2004). Ca^{++} gradients may also affect the behavior of negative cells of *D. discoideum* (Korohoda *et al.*, 2002). Hence, a variety of human cell types, like *D. discoideum* amoebae, translocate through environments containing different or changing concentrations of soluble Ca^{++}.

Extracellular Ca^{++} can affect the behavior of a cell in two ways. First, it can do so by regulating the intracellular concentration of free cytosolic Ca^{++}, the source of which can be bound Ca^{++} stores (Berridge, 2005; Berridge *et al.*, 2003; Oh-Hora *et al.*, 2008) and/or extracellular Ca^{++} (Berridge, 2005; Berridge *et al.*, 2003; Taylor, 2002; Wheeler and Brownlee, 2008; Fisher and Wilczynska, 2006; Lombardi *et al.*, 2008). Second, extracellular Ca^{++} can affect behavior through Ca^{++} receptors (Clark *et al.*, 2008; Hofer and Brown, 2003; Sharan *et al.*, 2008; Martinac *et al.*, 2008) that activate signaling pathways. These pathways may or may not affect the concentration of free cytosolic Ca^{++} (Clapham, 2007; Hofer and Brown, 2003).

Given the prevalence of Ca^{++} in the natural environment and the natural fluctuations in concentration experienced by free living organisms and cells migrating through the human body, it is remarkable how little we know about its effects on the basic motile behavior of a cell. Such information would facilitate not only our understanding of the role extracellular Ca^{++} might play in motility and chemotaxis in the natural life history of a cell, but also the relevance of behaviors identified under *in vitro* conditions, which in many cases include nonphysiological concentrations of extracellular Ca^{++}.

Here we have used 2D and 3D computer-assisted reconstruction and motion analysis systems (Soll, 1995, 1999; Soll *et al.*, 2003; Wessels *et al.*, 2006a, 2007; Heid *et al.*, 2005) to assess the effects of extracellular Ca^{++} on the basic motile behavior of *D. discoideum* amoebae and on chemotaxis in a spatial gradient of cAMP. We have also used fluorescent imaging methods to measure free cytosolic Ca^{++} and myosin II localization. Finally, we have tested whether extracellular K^+ and cAMP can substitute functionally for extracellular Ca^{++}. Our results demonstrate that there are two extracellular Ca^{++} concentration thresholds that affect different aspects of cell morphology, pseudopod formation, velocity, chemotaxis and the localization of myosin II in the cell cortex. Our results also demonstrate that extracellular K^+ and a cAMP gradient can partially substitute for extracellular Ca^{++}. Finally, our results indicate that extracellular Ca^{++}, K^+, and a cAMP gradient do not effect changes by similarly inducing increases in the general pool of free cytosolic Ca^{++}. Rather a model emerges in which the effects of extracellular Ca^{++}, K^+ and cAMP gradients on cell motility may be mediated through different signaling systems that converge to regulate the cortical localization of myosin II.

Materials and Methods

Strain maintenance and development

Frozen stocks of strain AX2 of *D. discoideum* were reconstituted every two weeks as previously described for experimental purposes (Wessels *et al.*, 2007). To obtain

aggregation-competent amoebae, cells were developed on filters according to methods previously described (Soll, 1979; Wessels *et al.*, 2006b, 2007). For analyses of basic motility and chemotaxis, cells were harvested from filters at the onset of aggregation (Soll, 1987), when velocity and chemotactic responsiveness under these conditions were maximum (Varnum *et al.*, 1986). Harvested cells were washed three times in a tricine buffer solution (TB: 5 mM tricine buffer, 5 mM KCl, pH 7.0) (Gardner, 1969; Böhme *et al.*, 1987; Wick *et al.*, 1978), then suspended in one of the following test solutions: TB alone, TB containing 5 mM EGTA [glycol-bis (1-aminoethylether)-N, N, N^1, N^1-tetra acetic acid], or TB containing varying concentrations of $CaCl_2$. TB does not contain phosphate, which precipitates Ca^{++} at high concentrations. TB had previously been shown to contain approximately 380 nM Ca^{++} (Buman *et al.*, 1984). In select experiments, cells were washed and resuspended in the buffered salt solution "LPS" (Sussman, 1987), which we will refer to as "BSS" (Soll, 1987). BSS contains 20 mM KCl, 2.5 mM $MgCl_2$, 20 mM KH_2PO_4 and 5 mM Na_2HPO_4, pH 6.4. The major cation in BSS was, therefore, 40 mM K^+. BSS contained no added Ca^{++}.

Analysis of basic motile behavior

Cells in a test solution were distributed at low density on the glass coverslip wall of a Sykes-Moore perfusion chamber (Bellco Glass, Vineland, NJ) (Varnum *et al.*, 1986), and incubated for one hour in that test solution prior to perfusion and analysis. The density was adjusted so that cells could crawl without contacting one another. Cells were perfused with test solution at a rate that resulted in turnover of chamber volume once every 15 sec, to exclude conditioning of the microenvironment. After 5 min of perfusion, cell behavior was videorecorded for 10 min.

Analysis of chemotaxis

Cells incubated for 1 hr in test solution were dispersed on the bridge of a plexiglass chamber (Varnum and Soll, 1984) designed after that of Zigmond (1977). The cell density was adjusted so that cells crawled during periods of analysis without contacting one another. Gradients were then generated by adding test solution without the chemoattractant cAMP to a trough on one side of the bridge and test solution with 10^{-6} M cAMP to a trough on the other side, according to methods previously described (Varnum and Soll, 1984). Cells were videorecorded beginning five minutes after solutions were added to the troughs.

DIAS analysis

For 2D studies of behavior, cells were video recorded through a bright-field 20× objective and motion-analyzed with 2D-DIAS software (Soll, 1995; Soll and Voss, 1998; Wessels *et al.*, 2006a). For 3D studies, cells were optically sectioned and reconstructed with 3D-DIAS software as previously described (Soll *et al.*, 2000, 2007; Zhang *et al.*, 2003; Wessels *et al.*, 1998, 2007; Heid *et al.*, 2002, 2005). Briefly, 60 optical sections were obtained in a two second period in the z-axis, and this process repeated every five seconds. Perimeters in each set of sections were outlined, pseudopods, which contained non-particulate cytoplasm, were discriminated from the cell body by drawing an interface line, and outlines converted to beta-spline representations. Velocity and turning parameters were based primarily on the position of the cell centroid, and shape parameters on the beta spline representations of the cell perimeter (Soll, 1995; Soll and Voss, 1998). Only cells with instantaneous velocities ≥ 3 μm per min were analyzed, since this has been found to represent on average a threshold for actual cellular translocation (Wessels *et al.*, 2000). Except for those treated with 5 mM EGTA, over 80% of all test populations meet this criterion.

Myosin staining

Myosin II was stained with anti-myosin II antibody (Burns *et al.*, 1995), a generous gift from Arturo de Lozanne of the University of Texas, Austin. The methods for staining were similar to those previously described (Wessels *et al.*, 1989, 2007), with the addition of an antigen retrieval step (Daniels *et al.*, 2006). Line profiles of grey scale intensity were obtained by general methods previously described (Wessels *et al.*, 2004, 2006b), using a Biorad Radiance 2100 MP laser scanning confocal microscope and software. Pixel intensity was monitored along a zigzag track that crossed the width of each cell at a slight angle from the anterior to posterior end approximately 10 to 15 times, extending outside the cell edge in each zigzag scan. The scans were processed using Zeiss LaserSharp™ software.

Measurements of cytosolic Ca^{++}

Fifty μl of cells (2×10^7 cells/ml) were washed once in ice-cold electroporation buffer (EB: 13 mM KH_2PO_4, 4 mM Na_2HPO_4 with KH_2PO_4 to pH 6.0), and resuspended in 20 μl of EB containing 1 mM $CaCl_2$ and 1 mg per ml of Fura-2-dextran (Invitrogen, Carlsbad, CA), which has been shown to stain free Ca^{++} selectively in the cytosol (Schlatterer *et al.*, 1992; Sonnemann *et al.*, 1997). This and all subsequent steps were performed in the presence of monochromatic red light to minimize loss of Fura-2-dextran fluorescence. The suspension was electroporated in a 0.2 cm Gap ice-cold electroporation cuvette (Biorad, Richmond, CA) at 850V, 3 μF and 200Ω. The time constant under these conditions was 0.6 seconds. Electroporation efficiency has been demonstrated to be independent of developmental time up to 7 hr and Fura-2-dextran has been shown to remain in a cell after electroporation throughout subsequent development (Sonnemann *et al.*, 1997). Immediately after electroporation, 80μl of EB containing 5 mM $MgCl_2$ were added to the cells to induce pore closure. Cells were incubated on ice for 10 min and then washed in EB. For measurements in the absence of cAMP, the cell pellet was resuspended in 70 μl of EB, 8 μl of it placed in a Sykes-Moore chamber, and incubated for 5 min for the cells to attach to the surface. For measurements in a spatial gradient of cAMP, cells were dispersed in test solution on a coverslip positioned on the bridge of a plexiglass gradient chamber (Varnum and Soll, 1984) designed after that of Zigmond (1977), and incubated for one hour prior to filling the troughs to generate a gradient as described previously. Preparations were analyzed through a Bio-Rad Radiance 2100MP Multiphoton/Confocal Microscope equipped with a Nikon S Fluor 1.30 40× oil objective. Three neutral density filters were placed in the light path. Cells were excited at 800 nm (Wokosin *et al.*, 2004). Emission was selected by a green filter (HQ 450/80; HQ 515/30; Dichroic 495 DCXR). Images were processed using Zeiss LaserSharp™ software and subsequently converted into QuickTime movies. The files were analyzed for grayscale intensity using the luminescence option of 2D-DIAS software (Wessels *et al.*, 2006a, 2007).

Results

The effects of $CaCl_2$ on cell motility

Since *D. discoideum* amoebae release the chemoattractant cAMP in response to cAMP in the process of signal relay (Shaffer, 1975; Bonner *et al.*, 1969; Konijn *et al.*, 1969; Alcantara and Monk, 1974; Gerisch *et al.*, 1975; Tomchik and Devreotes, 1981), cells in undisturbed culture can signal one another. To assess the effects of extracellular calcium on basic cell motility in the absence of chemoattractant, analyses were performed at very low cell densities in a perfusion chamber in which the high rate of flow further prevented conditioning of the soluble microenvironment. All test solutions were made in 5 mM tricine buffer (TB), pH 7.0, which contained 5 mM KCl and approximately 380 nM $CaCl_2$ (Buman *et al.*, 1984). In TB + 5 mM EGTA (EGTA), TB + 0 mM $CaCl_2$ (0 mM $CaCl_2$), or TB + $CaCl_2$ ranging in concentration from 0.1 to 20 mM (0.1 to 20 mM $CaCl_2$), a majority of cells

(78 to 95%) exhibited average instantaneous velocities ≥ 3μm per minute, which we considered the defining threshold for a motile *D. discoideum* amoeba undergoing persistent translocation (Wessels *et al.*, 2000) (Figure 1A). The highest proportions of motile cells were consistently attained at 10 and 20 mM, and the lowest at 40 mM $CaCl_2$ (Figure 1A). The differences between the proportions in 5 and 10 mM $CaCl_2$ was significant ($p = 0.02$).

The average instantaneous velocity of cells in EGTA, 0 mM $CaCl_2$, 0.1 mM $CaCl_2$ and 5 mM $CaCl_2$, ranged from 6.5 to 7 μm per min (Figure 1B). In 10 mM $CaCl_2$, however, the average instantaneous velocity increased to 13.5 μm per min, a significant increase of 93% over that in 5 mM $CaCl_2$ ($p = 5 \times 10^{-5}$) (Figure 1B). At 20 mM $CaCl_2$, the instantaneous velocity remained high (11.5 μm per min), but at 40 mM $CaCl_2$, it decreased to 6 μm per min (Figure 2B). The highest proportions of cells with velocities ≥ 9 μm per min were achieved at 10 and 20 mM $CaCl_2$ (Figure 1C). Positive flow, an area displacement measurement that computes movement independently of the cell centroid (Soll, 1995), also reached maximum values at 10 and 20 mM $CaCl_2$ (Figure 1D). The difference in positive flow between 5 and 10 mM $CaCl_2$ was highly significant ($p = 2 \times 10^{-6}$).

The extracellular concentration of $CaCl_2$ also affected two parameters that reflected the frequency of turning, “directional persistence” and “directional change” (Soll, 1995). The average value for directional persistence, measured as the net distance between the first and last cell centroid divided by the total distance of the centroid track (Soll, 1995), was very low in EGTA, increased 2.7 fold in 0 mM $CaCl_2$, then increased by 50% between 0 and 0.1 mM $CaCl_2$ (Figure 1E). It then increased at a low but relatively constant rate between 0.1 to 40 mM $CaCl_2$ (Figure 1E). Directional change, measured as the average change in the angle of translocation (Soll, 1995), decreased gradually as the $CaCl_2$ concentration increased to 5 mM, then remained relatively stable between 5 and 40 mM $CaCl_2$ (Figure 1F). It is noteworthy that while velocity parameters exhibited a precipitous increase between 5 and 10 mM $CaCl_2$, the two parameters that reflected the frequency of turning reached near a maximum and minimum value, respectively, at lower extracellular $CaCl_2$ concentrations. It is also noteworthy that although the four measured velocity parameters decreased dramatically at 40 mM $CaCl_2$, the two turning parameters remained optimum.

The effects of $CaCl_2$ on velocity and turning were reflected in the perimeter tracks of translocating cells. In EGTA, the tracks were highly compacted (Figure 2A) and cell shapes amorphous, rather than elongate (Figure 2A, insert). In 0 mM $CaCl_2$, the tracks were longer and more directional (Figure 2B). Cell shape was still, however, relatively amorphous rather than elongate (Figure 2B, insert). In 5 mM $CaCl_2$, however, cell tracks were longer and more persistent (Figure 2C), and cell shapes more elongate (Figure 2C, insert). Finally, in 10 mM $CaCl_2$ (data not shown) and 20 mM $CaCl_2$ (Figure 2D, insert), the tracks reached maximum lengths and persistent, and cell shapes were maximally elongate (Figure 2D, insert).

The effects of $CaCl_2$ on shape, uropod formation and pseudopod formation

In previous computer-assisted studies of the behavior of cells in the absence of chemoattractant, it was observed that cytoskeletal and regulatory mutants exhibited reduced velocity, increased directional change and amorphous shapes that were associated with defects in the suppression of lateral pseudopod formation, especially from the posterior half of the cell body (Wessels *et al.*, 2000, 2007; Kumar *et al.*, 2004; Heid *et al.*, 2004, 2005; Falk *et al.*, 2003; Soll *et al.*, 2002; Chung and Firtel, 1999; Lee *et al.*, 2004). In 2D analyses, we found that cells migrating in EGTA, or in 0 and 0.1 mM $CaCl_2$, also exhibited similar characteristics (Figure 1, 2), suggesting that in low concentrations of $CaCl_2$, normal cells might also be defective in the suppression of lateral pseudopod formation.

To assess the effects $CaCl_2$ concentration on cell shape and pseudopod dynamics in the absence of chemoattractant, we used 3D-DIAS software to reconstruct cells. In both EGTA (data not shown) and 0 mM $CaCl_2$ (Figure 3A), the average shape of a cell was relatively amorphous, with multiple pseudopods protruding from around the entire perimeter of the cell body. The pseudopods were uniformly small, and formed on and off the substratum. At 5 mM $CaCl_2$, cells were slightly more elongate, but pseudopods still protruded from around the entire cell perimeter and were uniformly small (Figure 3B). In 10 mM (Figure 3C) and 20 mM (data not shown) $CaCl_2$, however, cells were more elongate, possessed only one or two pseudopods at any one time and formed new pseudopods almost exclusively from the anterior half of the cell.

In EGTA (data not shown), 0 mM $CaCl_2$ (Figure 3A) and 5 mM $CaCl_2$ (Figure 3B), cells did not form a tapered posterior uropod. The anterior-posterior axis of these cells could be deduced by two parameters, the translocation vector and the position of posterior tail fibers (Heid *et al.*, 2004), which were not reconstructed here. In 10 mM $CaCl_2$, cells elongated and exhibited a visible change in curvature ("junction") between the larger, more ellipsoid main cell body and the tapered uropod (Figure 3C). At concentrations greater than 10 mM, these morphological characteristics were retained.

To quantitate the effect of $CaCl_2$ on pseudopod dynamics, the frequency of lateral pseudopod formation was measured in 2D. A lateral pseudopod was defined as a new expansion zone emanating either from the posterior flanks of an already existing anterior pseudopod (Andrew and Insall, 2007), or from the flanks of the cell body (Wessels *et al.*, 1988). To be considered a lateral pseudopod, the expansion zone had to contain particle-free cytoplasm clearly demarcated from the particulate cytoplasma of the main cell body, and attain a minimum area that was ≥ 3.5 percent of the total cell area (Wessels *et al.*, 1988). At 0 and 5 mM $CaCl_2$, cells formed on average eight and seven lateral pseudopods per 10 minutes, respectively, and did so equally from the anterior and posterior halves of the cell body (Figure 4A). At 10 mM $CaCl_2$, the frequency of total pseudopod formation decreased by approximately one half and, the major decrease was along the posterior half of the cell (Figure 4A). The average cell continued to form lateral pseudopods in 20 to 40 mM $CaCl_2$ from the anterior half of the cell at a frequency (three per ten minutes) close to that in 0, 5 and 10 mM $CaCl_2$ (four per ten minutes) but exhibited a decrease in frequency from the particular half, like cells in 10 mM $CaCl_2$ (Figure 4A). These results demonstrated that a major behavioral defect of cells in $CaCl_2$ at concentrations ≤ 5 mM was the incapacity to suppress lateral pseudopod formation along the posterior, not anterior, half of the cell.

The effects of extracellular $CaCl_2$ on adhesion

There was, however, a paradox in the behavior of cells in 40 mM $CaCl_2$. Although the shape of the cell body, the formation of the uropod, turning parameters (*i.e.*, directional persistence and directional change) and the suppression of lateral pseudopod formation in 40 mM $CaCl_2$ were similar to those in 10 mM $CaCl_2$, all velocity parameters decreased dramatically. An analysis of plating efficiency revealed that the majority of cells incubated in 40 mM $CaCl_2$ adhered to the chamber wall, as did a majority in 10 and 20 mM $CaCl_2$ (data not shown). 3D-DIAS reconstructions, however, revealed that at 10 and 20 mM $CaCl_2$, cells adhered to the substratum along their entire cell body and uropod, but at 40 mM $CaCl_2$ (data not shown) and at 80 mM $CaCl_2$ (Figure 3D), cells adhered to the substratum only by their uropod. Surprisingly, these latter cells still translocated in a persistent fashion, but at roughly half the velocity of cells in 10 mM $CaCl_2$ (Figure 1B). These results demonstrated that the anterior two-thirds of a cell (the main cell body) adhered to the glass substratum through Ca^{++}-sensitive adhesion sites, whereas the uropod adhered through Ca^{++}-insensitive adhesion sites.

The effects of $CaCl_2$ in a cAMP gradient

The effects of $CaCl_2$ were also analyzed in a spatial gradient of the chemoattractant cAMP. This condition was selected over global stimulation because the latter involves the rapid addition of a high concentration of cAMP uniformly to all points on the cell surface and, therefore, is not representative of the natural chemotactic signal which is in the form of an outwardly moving, nondissipating, relayed wave that crosses the cell over a seven minute period on average and includes both spatial and temporal gradients (Soll *et al.*, 2002). Whereas cells in a spatial gradient of cAMP undergo efficient locomotion and chemotaxis, cells globally stimulated with a high concentration of cAMP immediately cringe, stop translocating, dismantle their cortex and after several minutes partially rebound (Wessels *et al.*, 1989; Soll *et al.*, 2002).

As was the case in the absence of chemoattractant (Figure 1), the velocity parameters peaked at 10 and 20 mM $CaCl_2$ in a cAMP gradient (Figure 5A, B and C, respectively), and the turning parameters, reached near maxima and minima, respectively, at 5 mM (Figure 5E and F, respectively). There were, however, consistent differences between the effects of $CaCl_2$ in the absence and presence of a cAMP gradient. The average level of directional persistence at 0 and 5 mM $CaCl_2$ in a spatial gradient of cAMP (Figure 5E) was approximately two times higher than in the absence of cAMP (Figure 1E). In addition, directional change in 0 and 5 mM $CaCl_2$ in a spatial gradient of cAMP (Figure 5F) was lower than in the absence of cAMP (Figure 1F). These results demonstrated that a cAMP gradient in the absence of added $CaCl_2$ caused an increase in persistence, but did not affect velocity.

Analyses of cell shape and pseudopod formation further supported the conclusion that a cAMP gradient alone (*i.e.*, in 0 mM $CaCl_2$) induced several of the behavioral changes induced by $CaCl_2$, and, furthermore, that a cAMP gradient enhanced the effects of $CaCl_2$. In 0 mM $CaCl_2$, cells in a cAMP gradient (Figure 3E) were flatter and more elongate than those in the absence of chemoattractant (Figure 3A), and sometimes formed a small, but unstable uropod (Figure 3E). At 5 mM $CaCl_2$, these differences were accentuated. Cells in the absence of cAMP were amorphous, formed pseudopods around their entire perimeter and did not form a uropod (Figure 3B), but cells in a cAMP gradient were more elongate, formed a full-sized uropod and suppressed formation of lateral pseudopods (Figure 3F). The 3D reconstructions, therefore, suggested that the frequencies of lateral pseudopod formation in 0 and 5 mM $CaCl_2$ were lower in a cAMP gradient (Figures 3E and F, respectively) than they were in the absence of cAMP (Figures 3A and B, respectively). Measurements in 2D of the frequency of lateral pseudopod formation supported this suggestion. In a cAMP gradient generated in 0 mM $CaCl_2$, the frequency of lateral pseudopod formation (Figure 4B) was half that in 0 mM $CaCl_2$ in the absence of chemoattractant (Figure 4A). The major difference was in the frequency of pseudopods formed from the anterior half of the cell, 3.8 per 10 minutes in the absence of cAMP (Figure 4A) and 1.1 per 10 minutes in a spatial gradient of cAMP (Figure 4B), a 3.5 fold difference. The frequency of pseudopod formation along the posterior half of a cell was also lower in 0 mM $CaCl_2$ in a cAMP gradient, but not to the same extent as the frequency of anterior pseudopods (Figure 4A and B). In a cAMP gradient generated in ≥ 10 mM $CaCl_2$, the frequencies of anterior and posterior pseudopod formation approached a negligible frequency of zero per 10 minutes (Figure 4B), while in ≥ 10 mM $CaCl_2$ the absence of cAMP, the frequencies were approximately 2.7 and 0.8 per 10 minutes, respectively (Figure 4A). These results demonstrated that a cAMP gradient alone suppressed lateral pseudopod formation primarily in the anterior half of the cell, and that a cAMP gradient generated in ≥ 10 mM $CaCl_2$ completely suppressed lateral pseudopod formation, suggesting that the $CaCl_2$ and cAMP gradient effects might be additive.

The effects of calcium on the efficiency of chemotaxis

The effects of $CaCl_2$ were tested on two chemotaxis parameters, the average chemotactic index ("C.I."), which is the net distance traveled by the centroid of a cell up a spatial gradient of cAMP divided by total distance traveled in a 10 minute period, and the percent cells exhibiting a positive C.I. ("percent positive chemotaxis"). In previous computer-assisted studies of chemotaxis in a spatial gradient chamber, a C.I. value greater than +0.10 and a percent positive chemotaxis value greater than 60% have consistently provided thresholds for positive chemotactic responses. C.I. values increasing from +0.11 to +1.00, and percent positive chemotaxis values increasing from 61 to 100%, reflected increasing levels of chemotactic efficiency (Wessels *et al.*, 2004, 2007). For cells in a spatial gradient of cAMP containing 5mM EGTA, the average C.I. was less than +0.1 (Figure 5G) and the percent positive chemotaxis was very close to 60% (Figure 5H), indicating no chemotactic response. At 0 and 0.1 mM $CaCl_2$, however, the C.I.'s increased to +0.33 and +0.34, respectively, and the percent positive chemotaxis to 84 and 82%, respectively (Figure 5G and H, respectively), values reflecting a moderate positive chemotactic response. At 5 mM $CaCl_2$, however, the C.I. increased to +0.70, and the percent positive chemotactic index increased to 100% (Figure 5G and H, respectively), reflecting extremely efficient chemotaxic responses. These parameters remained high at 10, 20 and 40 mM (Figure 5G, H). The change in $CaCl_2$ concentration that caused the largest increase in chemotactic efficiency was from 0.1 to 5 mM (Figure 5G and H), the same concentration changed that caused the greatest increase in directional persistence (Figure 5E), the greatest decrease in directional change (Figure 5F), and near maximum suppression of lateral pseudopod formation (Figure 4B).

At 40 mM $CaCl_2$, the chemotaxis parameters remained high (Figure 5G and H, respectively), even though all of the velocity measurements decreased (Figure 5A, B, C and D). At 60 and 80 mM $CaCl_2$, however, the average C.I. decreased to +0.12 and +0.02, respectively, and the percent positive chemotaxis decreased to 65 and 45%, respectively (data not shown). As was observed at high $CaCl_2$ (≥ 40 mM) in the absence of chemoattractant (Figure 3D), the main cell body of a majority of cells did not adhere to the substratum; cells remained attached only by their uropods (Figure 3H).

The effects of $CaCl_2$ on myosin II localization

The majority of cell parameters that affected $CaCl_2$ in the absence of cAMP or in a cAMP gradient, including velocity, turning, the suppression of lateral pseudopod formation, cell shape and uropod formation, have been shown to be dependent upon the localization of myosin II in the posterior cortex of *D. discoideum* amoebae (Heid *et al.*, 2002; Catalano and O'Day 2008; Chung and Firtel, 1999; Bosgraaf and van Haastert, 2006; Jeon *et al.*, 2007; Zhang *et al.*, 2002, 2003; Shelden and Knecht, 1996; Laevsky and Knecht, 2003; Egelhoff *et al.*, 1993). We therefore entertained the hypothesis that $CaCl_2$ regulated these cell characteristics through the cortical localization of myosin II. This hypothesis was explored by staining cells incubated in 0 to 40 mM $CaCl_2$, in the absence of chemoattractant with anti-myosin II polyclonal antibody (Burns *et al.*, 1995). Stained cells were optically sectioned in the z-axis by multiphoton laser scanning confocal microscopy, and a projection image, derived from the center five sections (in the z-axis), analyzed for pixel intensity (Figure 6A through D). A zigzag scan of pixel intensity along the posterior-anterior axis crossed the width of the cell 15 times to points outside the cell edge (see inserts in Figure 6A through D). Pixel intensity was then plotted along the scan from the posterior to anterior end of a cell. For cells without distinct tapered uropods (*i.e.*, at 0 and 5 mM $CaCl_2$), the posterior end was identified by the location of tail fibers (Heid *et al.*, 2005). In Figure 6A through D, the broad peaks in each zigzag scan represented that portion through the cell. The points at the edges of each broad peak represented the intensity at the cell cortex, and the points in the

middle of each peak the cell interior. The troughs between each pair of broad peaks represented points outside the cell body.

In 0 mM $CaCl_2$ in the absence of cAMP, the average intensity of cortical staining was higher than that of interior staining (Figure 6A). There was no difference between the intensity of staining of the anterior and posterior cortex (Figure 6E, F); the ratio of posterior to anterior cortical staining was 1.0 (Figure 6G). At 5 mM $CaCl_2$, the average intensity of cortical staining of both the anterior and posterior halves of cells increased similarly by approximately 30% (Figure 6E, F). The ratio of posterior to anterior cortical staining was 1.0, just as it was at 0 mM $CaCl_2$ (Figure 6G). At 10 mM $CaCl_2$, however, while the average intensity of staining of the cortex of the anterior half of the cell, remained relatively unchanged from that in 5 mM $CaCl_2$, the average intensity of the posterior half increased by 50% (Figure 6E, F). The ratio of posterior to anterior cortical staining increased from 1.0 in 5 mM $CaCl_2$ to 1.6 in 10 mM $CaCl_2$ (Figure 6G). The absolute intensity increased slightly and the proportion decreased slightly between 10 and 40 mM $CaCl_2$ (Figure 6E, F, G). Together these results indicated that in the absence of cAMP, increasing the extracellular concentration of $CaCl_2$ to 5 mM led to a general increase in cortical myosin II in both the anterior and posterior half of a cell, but an increase in concentration to 10 mM or higher caused a further and selective increase in posterior, but not anterior, cortical localization. It should be noted that the differential increase in posterior but not anterior cortical myosin II was caused by an increase in the concentration of $CaCl_2$ from 5 to 10 mM in the absence of cAMP, the same increase in $CaCl_2$ that caused cell elongation, formation of the uropod, lateral pseudopod repression in the posterior half of a cell and an increase in velocity in the absence of chemoattractant.

Cells in a cAMP gradient generated in 0 mM $CaCl_2$ exhibited changes in turning and lateral pseudopod suppression that were induced by 5 mM $CaCl_2$ in the absence of cAMP, and cells in a cAMP gradient generated in 5 mM $CaCl_2$ exhibited many of the changes that were induced by 10 mM $CaCl_2$ We hypothesized that if $CaCl_2$ affected behavior by inducing myosin II localization in the cell cortex, then a cAMP gradient generated in 0 mM $CaCl_2$ should induce a general increase in myosin II localization throughout the entire cortex, as was the case for 5 mM $CaCl_2$ in the absence of cAMP, and a cAMP gradient generated in 5 mM $CaCl_2$ should induce a further selective increase in myosin II in the cortex of the posterior half of the cell, as was the case for 10 mM $CaCl_2$ in the absence of cAMP (Figure 6). These predictions were supported by staining experiments with anti-myosin II heavy chain antibody analyzed in the same fashion as the cell in Figure 6. For cells in a cAMP gradient in 0 mM $CaCl_2$, there was a two to three fold increase in general cortical staining when compared to parallel stained cells in 0 mM $CaCl_2$ in the absence of cAMP (Table 1). However, the ratio of anterior to posterior cortical staining was close to 1.0, as it was for cells in a cAMP gradient. In 5 mM $CaCl_2$ in a cAMP gradient, there was disproportionate staining in the posterior cortex of the cells, resulting in a ratio of anterior to posterior staining of 1.4 (Table 1). This contrasted, as predicted, with cells in 5 mM $CaCl_2$ in the absence of cAMP, which had a ratio very close to 1.0 (Figure 6), but was close to the ratio for cells in 10 mM $CaCl_2$ in the absence of cAMP (Figure 6). For cells in a cAMP gradient generated in 10 mM $CaCl_2$, the ratio was 1.7 (Table 1), very close to the ratio of cells in 10 mM $CaCl_2$ in the absence of cAMP (Figure 6). These results are consistent with the hypothesis that both extracellular Ca^{++} and cAMP effect changes in behavior by inducing an increase in myosin II localization in the general cell cortex, and a further selective increase in the posterior cortex. They also are consistent with the suggestion that the effects of cAMP and $CaCl_2$ may be additive, or that the former enhances the effects of the latter.

Extracellular K^+ can substitute for Ca^{++}

Although we have found here that increasing the extracellular concentration of $CaCl_2$ to 10 mM $CaCl_2$ induces changes in cell behavior that lead to highly efficient motility and chemotaxis, in past studies we routinely obtained efficient motility and chemotaxis in a buffered salt solution (BSS) that did not include Ca^{++} as an added component. BSS in the absence of cAMP supported cell elongation, uropod formation, myosin localization in the posterior half of the cell body and efficient motility, and in a cAMP gradient BSS supported all of these characteristics plus relatively efficient chemotaxis (Varnum *et al.*, 1986; Wessels *et al.*, 2004, 2006b, 2007; Zhang *et al.*, 2002, 2003; Heid *et al.*, 2004; Stepanovic *et al.*, 2005). BSS was originally formulated by Sussman and colleagues (Sussman, 1987) and referred to by then as "lower pad solution" (LPS). It contained 40 mM K^+, 10 mM Na^+ and 2.5 mM Mg^{++}. A comparison between data we previously obtained for Ax2 cells in BSS in the absence of cAMP (Wessels *et al.*, 2007) and data obtained here for Ax2 cells in 10 mM $CaCl_2$ revealed that the velocity parameters in BSS were consistently reduced and the frequency of pseudopod formation in the anterior half of the cell in BSS consistently higher (data not shown). Cells undergoing chemotaxis in a cAMP gradient generated in BSS also exhibited velocity parameters slightly lower than in a cAMP gradient generated in 20 mM $CaCl_2$ (Figure 7A through C). The chemotactic indices, however, were comparable (Figure 7D). We hypothesized that K^+, the major cation in BSS, might be responsible (*i.e.*, might substitute for extracellular Ca^{++}), especially since previous studies had shown in a variety of cell types that extracellular K^+ induced the release into the cytosol of stored Ca^{++} (Corrales *et al.*, 2005; Miyauchi *et al.*, 1990; Roberts *et al.*, 1984). We tested whether the motility and chemotaxis parameters of cells in a cAMP gradient generated in 40 mM KCl in TB were similar to those in a gradient generated in BSS. We found that they were highly similar (Figure 7A through D). Velocity parameters in 20 and 60 mM KCl, however, were reduced (Figure 7A, B), indicating that 40 mM KCl was optimum. Staining with anti-myosin II heavy chain antibody demonstrated that 40 mM KCl in a cAMP gradient induced a general increase in cortical staining, with further selective staining in the posterior cortex (Table 1). The ratio of posterior to anterior cortical staining, however, was 1.30 ± 0.21 (Table 1), which was lower than the ratio of 1.58 obtained in a cAMP gradient generated in 10 mM $CaCl_2$ (Figure 6G). NaCl at a concentration of 10 mM in TB, the concentration in BSS did not substitute for 10 mM $CaCl_2$ (data not shown), and NaCl at 20 mM was inhibitory to motility and chemotaxis (Figure 7A through D).

We next tested whether the divalent cation Mg^{++}, the concentration of which is 2.5 mM in BSS, could substitute for Ca^{++}. In TB + 2.5 mM $MgCl_2$, behavioral parameters were similar to those in TB + 0 mM $CaCl_2$ (data not shown), and in TB + 20 mM $MgCl_2$, motility and chemotaxis were inhibited (Figure 7E through H). $MnCl_2$ and $ZnCl_2$ at 20 mM were also inhibitory to motility and chemotaxis (Figure 7E through H). These results supported the conclusion that the monovalent cation K^+ was the component of BSS that supported efficient motility and chemotaxis.

Finally, we tested whether pH, which was maintained at 7.0 in the experiments reported here, affected motility and chemotaxis parameters. Within a measured range of 6.2 to 8.8, pH 7 proved optimum for velocity parameters (Figure 7I, J); both directional persistence and chemotaxis were insensitive to pH in that range (Figure 7K and L, respectively).

Intracellular Ca^{++}

Extracellular Ca^{++} has been shown to affect the level of free cytosolic Ca^{++} in a variety of cell types, including *D. discoideum* (Clapham *et al.*, 2001, 2007; Berridge *et al.*, 2003; Malchow *et al.*, 1996; Berridge, 2005; Clark and Petty, 2008; Fisher and Wilczynska, 2006; Taylor, 2002; Wheeler and Brownlee, 2008). We therefore considered the hypothesis that

the effects of extracellular Ca^{++} on cell behavior and on the cortical localization of myosin II were mediated through changes in the concentration of free cytosolic calcium. If true, then increasing the concentration of extracellular $CaCl_2$ from 0 to 10 mM, a maximum effect on behavior, should also increase the concentration of free cytosolic Ca^{++} to a maximum, and increasing the concentration to 20 and 40 mM of $CaCl_2$ should have no further effect on free cytosolic Ca^{++}. To measure free cytosolic Ca^{++}, cells were loaded with the indicator Fura-2-dextran. Cells of each treated population were then analyzed by fluorescence imaging methods for the relative concentration of free cytosolic Ca^{++} when incubated in 0, 5, 10 and 40 mM $CaCl_2$. The relative concentration was calculated in each of five independent experiments by taking the fluorescent intensity at 0 mM $CaCl_2$ to be 0 and the highest individual cell intensity at 10 or 40 mM $CaCl_2$ to be 100. Intermediate intensities were converted to intensities between 1 and 100%. Comparisons were made only within a single experiment in which fractions of a common pool of cells loaded with Fura-2-dextran were compared in different test solutions. In each of three or more experiments, the maximum relative concentration of free cytosolic Ca^{++} was obtained at 10 mM extracellular $CaCl_2$. The mean relative free cytosolic concentration at 5 mM $CaCl_2$ was 31 ± 12%, and at 10 mM, 98 ± 3% (Figure 8A). At 40 mM, it was 92 ± 8% (Figure 8A). These results demonstrated that, as predicted, extracellular Ca^{++} regulated the intracellular concentration of free cytosolic Ca^{++}, and that 10 mM extracellular Ca^{++} induced a maximum increase in free cytosolic Ca^{++}.

If extracellular Ca^{++} exerts its control on cell behavior by inducing an increase in free cytosolic Ca^{++}, then one would expect 40 mM K^+, which substitutes for extracellular Ca^{++}, to induce a similar increase in free cytosolic Ca^{++}. The results, however, did not support this prediction. Although KCl induced an increase in free cytosolic Ca^{++}, the mean relative concentration was only approximately one fourth that induced by 10 mM $CaCl_2$ (Figure 8B). This level of free cytosolic Ca^{++} was close to that induced by 5 mM $CaCl_2$ (Figure 8A) (p value was > 0.05). An extracellular concentration of 5 mM $CaCl_2$, however, effected a far less complete behavioral response than 40 mM KCl.

Based on similar logic, one would expect a spatial gradient of cAMP generated in 0 mM $CaCl_2$ to have a very small effect on the concentration of intracellular Ca^{++}. The results again did not support this prediction. In a spatial gradient of cAMP in 0 mM $CaCl_2$, the mean relative concentration of free cytosolic Ca^{++} for six independent experiments (Figure 8C, open circles) was 50% higher than that caused by in 10 mM $CaCl_2$ in the absence of chemoattractant (Figure 8C, closed circles). If the concentration of the cytosolic Ca^{++} regulated myosin II localization and the subsequent behavioral change, then one would have expected a cAMP gradient to induce a cytosolic Ca^{++} concentration for below that induced by 10 mM $CaCl_2$.

Discussion

$CaCl_2$ in the absence of cAMP

In 0 mM $CaCl_2$, cells were amorphous, extended small pseudopods from all surfaces of the cell body, did not form a uropod, and moved at reduced velocities and reduced persistence. Two concentration thresholds of $CaCl_2$ were identified that regulated different sets of these parameters. A concentration of 5 mM induced a maximum increase in persistent translocation (*i.e.*, a decrease in the frequency of turning), but had no measurable effect on speed, shape, lateral pseudopod dynamics or uropod formation. A concentration of 5 mM $CaCl_2$ also induced a general increase in the localization of myosin II throughout the cell cortex. Since increased cortical localization of myosin II causes an increase in cortical tension (Egelhoff *et al.*, 1996), one might assume that the increase in persistent translocation in 5 mM $CaCl_2$ might be a result of the general increase in myosin II localization and a

general increase in cortical tension. The absence of an apparent effect by 5 mM $CaCl_2$ on lateral pseudopod dynamics was, however, paradoxical, since a number of studies suggested that a decrease in the frequency of turning was usually associated with a decrease in lateral pseudopod formation (Soll *et al.*, 2002; Varnum-Finney *et al.*, 1987; Stites *et al.*, 1998; Wessels *et al.*, 1994, 2000, 2007; Shutt *et al.*, 1995). Since lateral pseudopods that touch the substratum are more prone to initiate sharp turns than lateral pseudopods that do not touch the substratum (Wessels *et al.*, 1994), one would expect the lateral pseudopods formed at 0 mM $CaCl_2$ to be primarily in contact with the substratum and the ones formed at 5 mM $CaCl_2$ to be off the substratum. Side views of 3D reconstructions of cells in 0 and 5 mM $CaCl_2$ revealed little difference (Figure 3B). The majority at both concentrations were in contact with the substratum. The difference in persistence between cells in 0 and 5 mM $CaCl_2$, therefore, remains an enigma.

The second concentration threshold that affected behavior was 10 mM $CaCl_2$. This concentration induced a dramatic increase in speed, cell elongation, formation of a distinct uropod and selective suppression of lateral pseudopod formation along the posterior half of the cell body. A 10 mM $CaCl_2$ had only a small additional effect over that of 5 mM $CaCl_2$ on turning parameters. A concentration of 10 mM $CaCl_2$ induced a further increase in cortical myosin localization, but in contrast to the increase induced at 5 mM $CaCl_2$, the increase was disproportionate in the posterior half of the cell. Given the role cortical myosin II plays in cortical tension (Egelhoff *et al.*, 1996; Girard *et al.*, 2006; Pasternak *et al.*, 1989; Yumura and Uyeda, 2003), we again suggest that the selective increase of myosin II localization in the posterior cortex may play a role in uropod formation and the selective suppression of lateral pseudopod formation along the posterior half of the cell (Heid *et al.*, 2004; Wessels *et al.*, 2007; Catalano and O'Day, 2008; Bosgraaf and van Haastert, 2006). One might also consider the possibility that an increase in cortical tension in the posterior half of a cell may play a role in elongation and in the associated increase in velocity.

Increases in free cytosolic Ca^{++} were also induced at the two $CaCl_2$ concentration thresholds, a relative increase of 30% at 5 mM and a maximum increase of 100% at 10 mM. Increasing the extracellular concentration to 40 mM, had no further effect on the concentration of free cytosolic Ca^{++}. Since Ca^{++} has been shown to inactivate a kinase responsible for phosphorylating the myosin II heavy chain (Maruta *et al.*, 1983), and phosphorylation causes myosin II to depolymerize and exit the cortex (Egelhoff *et al.*, 1993; Kuczmarski and Spudich, 1980; Kolman *et al.*, 1996; Moores *et al.*, 1996; Wessels *et al.*, 1988; Heid *et al.*, 2004), the possibility arises that an increase in free cytosolic Ca^{++} induced by extracellular $CaCl_2$ favors an increase in cortical localization and cortical tension. A simple model, therefore, can be formulated in which extracellular Ca^{++} causes an increase in the concentration of free cytosolic Ca^{++}, which inactivates the major myosin II heavy chain kinase, favoring cortical localization of myosin II. General cortical localization of myosin II, which is induced by 5 mM $CaCl_2$, suppresses turning, and selective posterior localization, which is induced by a further increase in the $CaCl_2$ concentration to 10 mM, causes changes in velocity, cell shape, uropod formation and selective suppression of posterior pseudopod formation. Clark *et al.* (2008) have suggested a related model based upon their work on mouse TRPM7, a cell surface cation channel highly permeable to Ca^{++}. This channel is fused to an α-kinase that phosphorylates the myosin IIA heavy chain. In this model, the authors propose that Ca^{++} influx through the channel in mouse neuroblastoma cells induces recruitment and hence phosphorylation of the actomyosin cytoskeleton. Activation leads to relaxation of the cytoskeleton, which increases spreading and adhesion. Hence the effect of extracellular Ca^{++} in this case may have the effect of dismantling the cortical cytoskeleton.

Extracellular KCl substitutes for $CaCl_2$

We have found that 40 mM K^+ will substitute for $CaCl_2$. A comparison of the effects of 40 mM KCl and 10 mM $CaCl_2$ is presented in Table 2. Although it induces all of the changes that are induced by 10 mM $CaCl_2$, the level of induction of some of the parameters were not of the same magnitude. This was especially true for velocity parameters and pseudopod suppression. The capacity of extracellular K^+ to substitute for extracellular Ca^{++} was not surprising given that it had been demonstrated in a variety of cell types that extracellular K^+ causes an increase of free cytosolic Ca^{++} through release from bound stores (Roberts *et al.*, 1984;Miyauchi *et al.*, 1990;Corrales *et al.*, 2005), and that specific K^+ channels are sensitive to extracellular Ca^{++} (Ko *et al.*, 2008;Jackson, 2005). We found that 40 mM KCl in the absence of cAMP induced an increase in free cytosolic Ca^{++}, but to approximately one third the level caused by 10 mM $CaCl_2$. This observation did not fully support the simple hypothesis that the extracellular signal Ca^{++}, or K^+, induced cytoskeletal and behavioral changes by increasing free cytosolic Ca^{++}. If that were simply the case, then 40 mM K^+ should induce an increase in free cytosolic Ca^{++} close to the level induced by 10 mM $CaCl_2$, not 5 mM $CaCl_2$, which does not cause many of the effects of 40 mM KCl and 10 mM $CaCl_2$.

The specificity of Ca^{++} and K^+ as alternative extracellular stimuli suggests that each may function through a specific surface receptor or channel. Receptors or channels for both cations have been identified in a variety of cell types (Clark *et al.*, 2008; Hofer and Brown, 2003; Sharan *et al.*, 2008; Martinac *et al.*, 2008). Two *D. discoideum* genes have been identified that are homologous to the human genes for TRP channels for Ca^{++}, which facilitate chemosensing in axons (Martinac *et al.*, 2008). Furthermore, a metabotropic glutamate receptor has been identified in *D. discoideum* (Taniura *et al.*, 2006). These receptors have sequence homologies with calcium receptors (Brown *et al.*, 1993) and pheromone receptors (Herrada and Dulac, 1997; Matsunami and Buck, 1997). Potential K^+ channels have also been identified in *D. discoideum* by patch-clamp analyses (Muller and Hartung, 1990; Muller *et al.*, 1986). The possible roles of these surface molecules in the cellular responses to extracellular Ca^{++} and K^+ are now under investigation.

cAMP gradients

In addition to extracellular K^+, we demonstrated here that spatial gradients of cAMP selectively induced some of the same changes induced by $CaCl_2$ and KCl. A comparison of the effects of extracellular K^+, Ca^{++} and a cAMP gradient is presented in Table 2. Free cytosolic Ca^{++} had previously been demonstrated to increase in a population of aggregating cells at the time of cAMP signaling, suggesting that cAMP stimulated an increase in the steady state level of free cytosolic Ca^{++} (Saran *et al.*, 1994). Subsequent studies revealed that global stimulation with cAMP caused a spike in free cytosolic Ca^{++} (Yumura *et al.*, 1996;Schlatterer *et al.*, 1994;Abe *et al.*, 1988;Nebl and Fisher, 1997;Unterweger and Schlatterer, 1995). The abnormal addition of a high concentration of cAMP to aggregation-competent *D. discoideum*, however, causes a dramatic reduction in cell motility, rounding-up and an abnormal, transient increase in F-actin and myosin localization throughout the entire cell cortex (Wessels *et al.*, 1989,2000;Soll *et al.*, 2002;Zhang *et al.*, 2003;Stepanovic *et al.*, 2005). This makes it difficult to ascertain the relevance of the spike in free Ca^{++} caused by global stimulation given that the natural cAMP signal is in the form of a wave (Loomis, 2008;Vicker and Grutsch, 2008;Tomchik and Devreotes, 1981;Soll *et al.*, 2002). Traynor *et al.* (2000) demonstrated through mutant analysis that the spike does not occur upon global cAMP stimulation in the null mutant of the inositol 1,4,5-triphosphate ($InsP_3$) receptor-like gene, iplA, yet this mutant undergoes normal chemotaxis in a spatial gradient of cAMP, suggesting that the spike is not essential for normal chemotaxis. Schaloske *et al.* (2005), however, presented evidence indicating that Ca^{++}-regulation does occur under

specific conditions in the iplA mutant. The general consensus is that the role of the spike remains elusive (Bagorda *et al.*, 2006).

Because of the ambiguities associated with global cAMP stimulation, we analyzed the effects of $CaCl_2$ on cells undergoing chemotaxis in a spatial gradient of cAMP. We have demonstrated that a spatial cAMP gradient generated in the absence of extracellular $CaCl_2$ caused a decrease in turning, suppression of anterior pseudopod formation, partial elongation, formation of an incipient but unstable uropod and general myosin II localization around the cell cortex. It also induced moderately efficient chemotaxis. When a spatial gradient of cAMP was generated in the presence of 10 mM $CaCl_2$, however, the velocity parameters increased to those obtained in 10 mM $CaCl_2$ in the absence of cAMP, turning was suppressed beyond the levels stimulated by 10 mM $CaCl_2$ in the absence of cAMP and chemotaxis became even more efficient (*i.e.*, the C.I. was twice that in a gradient in the absence of $CaCl_2$), suggesting that select Ca^{++} and cAMP effects were additive. Moreover, in 5 mM $CaCl_2$ in the absence of cAMP, there was a general increase in the cortical localization of myosin II, but when a cAMP gradient was generated in 5 mM $CaCl_2$, there was selective localization in the posterior cortex, again demonstrating additivity or enhancement.

If the simple hypothesis was correct that 10 mM $CaCl_2$ stimulated behavioral changes by increasing free cytosolic Ca^{++} to a threshold level which in turn induced selective localization of myosin II in the posterior cell cortex and subsequent behavioral changes, then a cAMP gradient generated in the absence of $CaCl_2$ should induce a level of free cytosolic calcium far below that threshold. The reason for this is that a cAMP gradient alone causes submaximal effects on behavior and does not induce differential localization of myosin II in the posterior cortex. Instead, we found that a cAMP gradient in 0 mM $CaCl_2$ induced an increase in free cytosolic Ca^{++} more than 30% higher than that induced by 10 mM $CaCl_2$. This result demonstrates that simply increasing free cytosolic Ca^{++} to a threshold level, in this case the level induced by 10 mM $CaCl_2$, is insufficient to induce the maximum increase in velocity, suppression of posterior pseudopod formation, formation of a full sized and stable uropod as well as selective localization of myosin II in the posterior cortex of the cell. When a spatial gradient was generated in 10 mM $CaCl_2$, all motility and chemotaxis parameters, and the localization of myosin II in the cortex, were equal to or greater than that in 10 mM $CaCl_2$ in the absence of cAMP. These results are more consistent with a model in which extracellular Ca^{++}, K^+ and cAMP signal surface receptors that activate signal transduction pathways that may not include a general increase in free cytosolic Ca^{++} as a component or second messenger.

Concluding remarks

We have, therefore, demonstrated that extracellular Ca^{++}, a major cation in the environment of most cells, regulates cell morphology, cell behavior and the organization of the cortical cytoskeleton. Extracellular K^+ can substitute for extracellular Ca^{++}, effecting common changes, but not quite to the same extent. In addition a spatial gradient of cAMP alone can effect only a few of the changes effected by extracellular Ca^{++}, and to levels below those induced by Ca^{++}. The specificity of Ca^{++} among common divalent cations, and the inability of Na^+ to substitute for K^+, suggest that, as is the case for cAMP, extracellular Ca^{++} and K^+ effect common behavioral changes through independent Ca^{++} and K^+ receptors, or channels. Although we initially assumed that the three signals would all affect changes in the cytoskeleton and behavior by increasing free cytosolic Ca^{++}, our results do not support so simple a model. The observations that a cAMP gradient alone induces a larger increase in free cytosolic Ca^{++} than 10 mM $CaCl_2$, but does not induce most of the major changes in morphology and behavior that 10 mM $CaCl_2$ induces, leads us to propose that both extracellular Ca^{++} and K^+ induce changes through receptors that activate signal transduction

pathways, just as cAMP effects cell behavior through receptor-mediated signal transduction pathways (Garcia and Parent, 2008; Kay *et al.*, 2008; Janetopoulos and Firtel, 2008; Andrews and Insall, 2007; Veltman *et al.*, 2008; Iglesias and Devreotes, 2008). The transduction of an extracellular Ca^{++} signal through such pathways has been demonstrated for the Ca^{++} receptor of the parathyroid and a variety of other cell types (Ramasamy, 2006; Hofer and Brown, 2003; Sharan *et al.*, 2008). Alternatively extracellular Ca^{++} and K^{+} may activate surface molecules that directly interact with the cytoskeleton, as is the case for TRPM7 (Clark *et al.*, 2008). Therefore, although we still believe that the downstream effects of extracellular Ca^{++} and K^{+} stimulation are commonly mediated at least in part through the regulation of myosin II localization in the cell cortex, we do not believe that a common intermediate step is an increase in the general free cytosolic Ca^{++} pool. Our collective results, therefore, suggest a model in which extracellular Ca^{++}, K^{+} and cAMP, interacting with different receptors, activate common or separate signal transduction pathways. The common downstream effect of the three signals is an increase in myosin II localization in the cell cortex through the regulation of the phosphorylated state of the myosin II heavy chain (Yumura *et al.*, 2005; Heid *et al.*, 2005; Egelhoff *et al.*, 1996; Luck-Vielmetter *et al.*, 1990; Rahmsdorf *et al.*, 1979; Malchow *et al.*, 1981). The general increase in cortical myosin and the differential increase in the posterior cortex in turn play fundamental roles in elongation, uropod formation and pseudopod formation. These changes are basic to the efficiency of the basic motile behavior of a cell, and this in turn increases the efficiency of chemotaxis in a spatial gradient cAMP (Soll *et al.*, 2002). Although this model is oversimplified and does not explain the polar effects of signal induction, such as the selective increase in myosin II in the posterior half of a cell, or the nature of the signal transduction machinery, it does provide a contextual framework for pursuing answers to these questions.

Acknowledgments

The authors are indebted to Arturo de Lozanne for his generous gift of anti-myosin antibody, to Christine Haddad, William Mosher, Martin Forde, Karyl Gerbeck and Benjamin Soll for technical help with outlining and Chantal Allmargot for help in confocal measurements of cytosolic Ca^{++}. This work was funded in part by National Institutes of Health grant HD-18577 and the Developmental Studies Hybridoma Bank at the University of Iowa, a national resource.

References

Abe T, Maeda Y, Iijima T. Transient increase of the intracellular Ca++ concentration during chemotactic signal transduction in Dictyostelium discoideum cells. Differentiation. 1988; 39(2):90–6. [PubMed: 2854083]

Alcantara F, Monk M. Signal propagation during aggregation in the slime mould Dictyostelium discoideum. J Gen Microbiol. 1974; 85(2):321–34. [PubMed: 4615133]

Andrew N, Insall RH. Chemotaxis in shallow gradients is mediated independently of PtdIns 3-kinase by biased choices between random protrusions. Nat Cell Biol. 2007; 9(2):193–200. [PubMed: 17220879]

Bagorda A, Mihaylov VA, Parent CA. Chemotaxis: moving forward and holding on to the past. Thromb Haemost. 2006; 95(1):12–21. [PubMed: 16543956]

Bangerth F. Calcium-Related Physiological Disorders of Plants. Annual Review of Phytopathology. 1979; 17(1):97–122.

Berridge MJ, Bootman MD, Roderick HL. Calcium signalling: dynamics, homeostasis and remodelling. Nat Rev Mol Cell Biol. 2003; 4(7):517–29. [PubMed: 12838335]

Berridge MJ. Unlocking the secrets of cell signaling. Annu Rev Physiol. 2005; 67:1–21. [PubMed: 15709950]

Beug H, Katz FE, Gerisch G. Dynamics of antigenic membrane sites relating to cell aggregation in Dictyostelium discoideum. J Cell Biol. 1973; 56(3):647–58. [PubMed: 4631665]

Böhme R, Bumann J, Aeckerle S, Malchow D. A high-affinity plasma membrane Ca++-ATPase in Dictyostelium discoideum: its relation to cAMP-induced Ca++-fluxes. Biochim Biophys Acta. 1987; 904(1):125–30. [PubMed: 2822110]

Bonner JT, Barkley DS, Hall EM, Konijn TM, Mason JW, O'Keefe G 3rd, Wolfe PB. Acrasin, Acrasinase, and the sensitivity to acrasin in Dictyostelium discoideum. Dev Biol. 1969; 20(1):72–87. [PubMed: 4307638]

Bosgraaf L, van Haastert PJ. The regulation of myosin II in Dictyostelium. Eur J Cell Biol. 2006; 85(9-10):969–79. [PubMed: 16814425]

Breitwieser GE. Extracellular calcium as an integrator of tissue function. Int J Biochem Cell Biol. 2008; 40(8):1467–80. [PubMed: 18328773]

Brown EM, Gamba G, Riccardi O, Lombardi M, Butters R, Kifor O, Sun A, Hediger MA. Cloning and characterization of an extracellular Ca(2+)-sensing receptor from bovine parathyroid. Nature. 1993; 366(6455):575–580. [PubMed: 8255296]

Bumann J, Wurster B, Malchow D. Attractant-induced changes and oscillations of the extracellular Ca ++ concentration in suspensions of differentiating Dictyostelium cells. J Cell Biol. 1984; 98(1): 173–8. [PubMed: 6323484]

Burns CG, Reedy M, Heuser J, De Lozanne A. Expression of light meromyosin in Dictyostelium blocks normal myosin II function. J Cell Biol. 1995; 130:605–612. [PubMed: 7622561]

Catalano A, O'Day DH. Calmodulin-binding proteins in the model organism Dictyostelium: a complete & critical review. Cell Signal. 2008; 20(2):277–91. [PubMed: 17897809]

Chung CY, Firtel RA. PAKa, a putative PAK family member, is required for cytokinesis and the regulation of the cytoskeleton in Dictyostelium discoideum cells during chemotaxis. J Cell Biol. 1999; 147(3):559–76. [PubMed: 10545500]

Clapham DE, Runnels LW, Strubing C. The TRP ion channel family. Nat Rev Neurosci. 2001; 2(6): 387–96. [PubMed: 11389472]

Clapham DE. Calcium signaling. Cell. 2007; 131(6):1047–58. [PubMed: 18083096]

Clark AJ, Petty HR. Observation of calcium microdomains at the uropod of living morphologically polarized human neutrophils using flash lamp-based fluorescence microscopy. Cytometry A. 2008; 73(7):673–8. [PubMed: 18496849]

Clark K, Middelbeek J, van Leeuwen FN. Interplay between TRP channels and the cytoskeleton in health and disease. Eur J Cell Biol. 2008; 87(8-9):631–40. [PubMed: 18342984]

Corrales A, Montoya GJ, Sutachan JJ, Cornillez-Ty G, Garavito-Aguilar Z, Xu F, Blanck TJ, Recio-Pinto E. Transient increases in extracellular K+ produce two pharmacological distinct cytosolic Ca ++ transients. Brain Res. 2005; 1031(2):174–84. [PubMed: 15649442]

Daniels KJ, Srikantha T, Lockhart SR, Pujol C, Soll DR. Opaque cells signal white cells to form biofilms in Candida albicans. Embo J. 2006; 25(10):2240–52. [PubMed: 16628217]

Dauer J, Chorover J, Chadwick O, Oleksyn J, Tjoelker M, Hobbie S, Reich P, Eissenstat D. Controls over leaf and litter calcium concentrations among temperate trees. Biogeochemistry. 2007; 86:175–187.

Day, E. The chemical elements in nature. George C. Harrap &Co; London UK: 1963.

Dodds, W. Freshwater Ecology: Concepts and Environmental Applications. Academia Press; 2002.

Egelhoff TT, Lee RJ, Spudich JA. Dictyostelium myosin heavy chain phosphorylation sites regulate myosin filament assembly and localization in vivo. Cell. 1993; 75(2):363–71. [PubMed: 7691416]

Egelhoff TT, Naismith TV, Brozovich FV. Myosin-based cortical tension in Dictyostelium resolved into heavy and light chain-regulated components. J Muscle Res Cell Motil. 1996; 17:269–274. [PubMed: 8793728]

Falk DL, Wessels D, Jenkins L, Pham T, Kuhl S, Titus MA, Soll DR. Shared, unique and redundant functions of three members of the class I myosins (MyoA, MyoB and MyoF) in motility and chemotaxis in Dictyostelium. J Cell Sci. 2003; 116(Pt 19):3985–99. [PubMed: 12953059]

Fisher PR, Wilczynska Z. Contribution of endoplasmic reticulum to Ca++ signals in Dictyostelium depends on extracellular Ca++ FEMS Microbiol Lett. 2006; 257(2):268–77. [PubMed: 16553863]

Garcia GL, Parent CA. Signal relay during chemotaxis. J Microsc. 2008; 231(3):529–34. [PubMed: 18755009]

Gardner RS. The use of tricine buffer in animal tissue cultures. J Cell Biol. 1969; 42(1):320–1. [PubMed: 5786986]

Gerisch G, Wick U. Intracellular oscillations and release of cyclic AMP from Dictyostelium cells. Biochem Biophys Res Commun. 1975; 65(1):364–70. [PubMed: 167769]

Girard KD, Kuo SC, Robinson DN. Dictyostelium myosin II mechanochemistry promotes active behavior of the cortex on long time scales. Proc Natl Acad Sci USA. 2006; 103:2103–2108. [PubMed: 16461463]

Godwin SL, Soltoff SP. Extracellular calcium and platelet-derived growth factor promote receptor-mediated chemotaxis in osteoblasts through different signaling pathways. J Biol Chem. 1997; 272(17):11307–12. [PubMed: 9111036]

Goldberg E, Broecker W, Gross M, Turekian K. Radioactivity in the Marine Environment. National Acad Sci Washington. 1971

Herrada G, Dulac CA. A novel family of putative pheromone receptors in mammals with a topographically organized and sexually dimorphic distribution. Cell. 1997; 90(4):763–773. [PubMed: 9288755]

Heid PJ, Voss E, Soll DR. 3D-DIASemb: a computer-assisted system for reconstructing and motion analyzing in 4D every cell and nucleus in a developing embryo. Dev Biol. 2002; 245(2):329–47. [PubMed: 11977985]

Heid PJ, Wessels D, Daniels KJ, Gibson P, Zhang H, Voss E, Soll DR. The role of myosin heavy chain phosphorylation in Dictyostelium motility, chemotaxis and F-actin localization. J Cell Sci. 2004; 117:4819–4835. [PubMed: 15340009]

Heid PJ, Geiger J, Wessels D, Voss E, Soll DR. Computer-assisted analysis of filopod formation and the role of myosin II heavy chain phosphorylation in Dictyostelium. J Cell Sci. 2005; 118(Pt 10): 2225–37. [PubMed: 15855234]

Hem, J. Study and Interpretation of the Chemical Characteristics of Natural Water. U.S. Government Printing Office; 1970.

Hem J. The study and interpretation of the chemical characteristics of natural water. USGS Water Supply Paper 2254. 1989

Hofer AM, Brown EM. Extracellular calcium sensing and signalling. Nat Rev Mol Cell Biol. 2003; 4(7):530–8. [PubMed: 12838336]

Iglesias PA, Devreotes PN. Navigating through models of chemotaxis. Curr Opin Cell Biol. 2008; 20(1):35–40. [PubMed: 18207721]

Jackson WF. Potassium channels in the peripheral microcirculation. Microcirculation. 2005; 12(1): 113–27. [PubMed: 15804979]

Janetopoulos C, Firtel RA. Directional sensing during chemotaxis. FEBS Lett. 2008; 582(14):2075–85. [PubMed: 18452713]

Jeon TJ, Lee DJ, Merlot S, Weeks G, Firtel RA. Rap1 controls cell adhesion and cell motility through the regulation of myosin II. J Cell Biol. 2007; 176(7):1021–33. [PubMed: 17371831]

Jeziorski A, Yan ND, Paterson AM, Desellas AM, Turner MA, Jeffries DS, Keller B, Weeber RC, McNicol DK, Palmer ME, et al. The widespread threat of calcium decline in fresh waters. Science. 2008; 322(5906):1374–7. [PubMed: 19039134]

Kay RR, Langridge P, Traynor D, Hoeller O. Changing directions in the study of chemotaxis. Nat Rev Mol Cell Biol. 2008; 9(6):455–63. [PubMed: 18500256]

Kindzelskii AL, Sitrin RG, Petty HR. Cutting edge: optical microspectrophotometry supports the existence of gel phase lipid rafts at the lamellipodium of neutrophils: apparent role in calcium signaling. J Immunol. 2004; 172(8):4681–5. [PubMed: 15067042]

Ko EA, Han J, Jung ID, Park WS. Physiological roles of K+ channels in vascular smooth muscle cells. J Smooth Muscle Res. 2008; 44(2):65–81. [PubMed: 18552454]

Kolman MF, Futey LM, Egelhoff TT. Dictyostelium myosin heavy chain kinase A regulates myosin localization during growth and development. J Cell Biol. 1996; 132(1-2):101–9. [PubMed: 8567716]

Konijn TM, van de Meene JG, Chang YY, Barkley DS, Bonner JT. Identification of adenosine-3′,5′-monophosphate as the bacterial attractant for myxamoebae of Dictyostelium discoideum. J Bacteriol. 1969; 99(2):510–2. [PubMed: 4309098]

Korohoda W, Madeja Z, Sroka J. Diverse chemotactic responses of Dictyostelium discoideum amoebae in the developing (temporal) and stationary (spatial) concentration gradients of folic acid, cAmP, Ca(2+) and Mg(2+). Cell Motil Cytoskeleton. 2002; 53(1):1–25. [PubMed: 12211112]

Kuczmarski ER, Spudich JA. Regulation of myosin self-assembly: phosphorylation of Dictyostelium heavy chain inhibits formation of thick filaments. Proc Natl Acad Sci U S A. 1980; 77(12):7292–6. [PubMed: 6452632]

Kumar A, Wessels D, Daniels KJ, Alexander H, Alexander S, Soll DR. Sphingosine-1-phosphate plays a role in the suppression of lateral pseudopod formation during Dictyostelium discoideum cell migration and chemotaxis. Cell Motil Cytoskeleton. 2004; 59(4):227–41. [PubMed: 15476260]

Laevsky G, Knecht DA. Cross-linking of actin filaments by myosin II is a major contributor to cortical integrity and cell motility in restrictive environments. J Cell Sci. 2003; 116(Pt 18):3761–70. [PubMed: 12890752]

Lee S, Rivero F, Park KC, Huang E, Funamoto S, Firtel RA. Dictyostelium PAKc is required for proper chemotaxis. Mol Biol Cell. 2004; 15(12):5456–69. [PubMed: 15483055]

Lombardi ML, Knecht DA, Lee J. Mechano-chemical signaling maintains the rapid movement of Dictyostelium cells. Exp Cell Res. 2008; 314(8):1850–9. [PubMed: 18359017]

Loomis WF. cAMP oscillations during aggregation of Dictyostelium. Adv Exp Med Biol. 2008; 641:39–48. [PubMed: 18783170]

Luck-Vielmetter D, Schleicher M, Grabatin B, Wippler J, Gerisch G. Replacement of threonine residues by serine and alanine in a phosphorylatable heavy chain fragment of Dictyostelium myosin II. FEBS Lett. 1990; 269(1):239–43. [PubMed: 2387408]

Malchow D, Böhme R, Rahmsdorf HJ. Regulation of phosphorylation of myosin heavy chain during the chemotactic response of Dictyostelium cells. Eur J Biochem. 1981; 117(1):213–8. [PubMed: 7262086]

Malchow D, Mutzel R, Schlatterer C. On the role of calcium during chemotactic signalling and differentiation of the cellular slime mould Dictyostelium discoideum. Int J Dev Biol. 1996; 40(1): 135–9. [PubMed: 8735922]

Martinac B, Saimi Y, Kung C. Ion channels in microbes. Physiol Rev. 2008; 88(4):1449–90. [PubMed: 18923187]

Maruta H, Baltes W, Dieter P, Marme D, Gerisch G. Myosin heavy chain kinase inactivated by Ca++/calmodulin from aggregating cells of Dictyostelium discoideum. Embo J. 1983; 2(4):535–42. [PubMed: 6313344]

Matsunami H, Buck LB. A multigene family encoding a diverse array of putative pheromone receptors in mammals. Cell. 1997; 90(4):775–784. [PubMed: 9288756]

McLaughlin, SB.; Wimmer, R. Tansley review no 104 Calcium physiology and terrestrial ecosystem processes. Cambridge: Cambridge University Press; 1999. p. 373-417.

Miyauchi A, Hruska KA, Greenfield EM, Duncan R, Alvarez J, Barattolo R, Colucci S, Zambonin-Zallone A, Teitelbaum SL, Teti A. Osteoclast cytosolic calcium, regulated by voltage-gated calcium channels and extracellular calcium, controls podosome assembly and bone resorption. J Cell Biol. 1990; 111(6 Pt 1):2543–52. [PubMed: 1703539]

Moores SL, Sabry JH, Spudich JA. Myosin dynamics in live Dictyostelium cells. Proc Natl Acad Sci U S A. 1996; 93(1):443–6. [PubMed: 8552657]

Muller U, Malchow D, Hartung K. Single ion channels in the slime mold Dictyostelium discoideum. Biochim Biophys Acta. 1986; 857(2):287–90. [PubMed: 18389567]

Muller U, Hartung K. Properties of three different ion channels in the plasma membrane of the slime mold Dictyostelium discoideum. Biochim Biophys Acta. 1990; 1026(2):204–12. [PubMed: 1696127]

Nebl T, Fisher PR. Intracellular Ca++ signals in Dictyostelium chemotaxis are mediated exclusively by Ca++ influx. J Cell Sci. 1997; 110(Pt 22):2845–53. [PubMed: 9427292]

Oh-Hora M, Yamashita M, Hogan PG, Sharma S, Lamperti E, Chung W, Prakriya M, Feske S, Rao A. Dual functions for the endoplasmic reticulum calcium sensors STIM1 and STIM2 in T cell activation and tolerance. Nat Immunol. 2008

Pasternak C, Spudich JA, Elson EL. Capping of surface receptors and concomitant cortical tension are generated by conventional myosin. Nature. 1989; 341:549–551. [PubMed: 2797182]

Rahmsdorf HJ, Malchow D, Gerisch G. Cyclic AMP-induced phosphorylation in Dictyostelium of a polypeptide comigrating with myosin heavy chains. FEBS Lett. 1979; 88(2):322–6. [PubMed: 206468]

Ramasamy I. Recent advances in physiological calcium homeostasis. Clin Chem Lab Med. 2006; 44(3):237–73. [PubMed: 16519596]

Randolph GJ, Ochando J, Partida-Sanchez S. Migration of dendritic cell subsets and their precursors. Annu Rev Immunol. 2008; 26:293–316. [PubMed: 18045026]

Roberts RL, Mounessa NL, Gallin JI. Increasing extracellular potassium causes calcium-dependent shape change and facilitates concanavalin A capping in human neutrophils. J Immunol. 1984; 132(4):2000–6. [PubMed: 6699404]

Saran S, Nakao H, Tasaka M, Iida H, Tsuji FI, Nanjundiah V, Takeuchi I. Intracellular free calcium level and its response to cAMP stimulation in developing Dictyostelium cells transformed with jellyfish apoaequorin cDNA. FEBS Lett. 1994; 337(1):43–7. [PubMed: 8276111]

Schaloske RH, Lusche DF, Bezares-Roder K, Happle K, Malchow D, Schlatterer C. Ca2+ regulation in the absence of the iplA gene product in Dictyostelium discoideum. BMC Cell Biol. 2005; 6(1): 13. [PubMed: 15760480]

Scherberich A, Campos-Toimil M, Ronde P, Takeda K, Beretz A. Migration of human vascular smooth muscle cells involves serum-dependent repeated cytosolic calcium transients. J Cell Sci. 2000; 113(Pt 4):653–62. [PubMed: 10652258]

Schlatterer C, Knoll G, Malchow D. Intracellular calcium during chemotaxis of Dictyostelium discoideum: a new fura-2 derivative avoids sequestration of the indicator and allows long-term calcium measurements. Eur J Cell Biol. 1992; 58(1):172–81. [PubMed: 1322818]

Schlatterer C, Gollnick F, Schmidt E, Meyer R, Knoll G. Challenge with high concentrations of cyclic AMP induces transient changes in the cytosolic free calcium concentration in Dictyostelium discoideum. J Cell Sci. 1994; 107(Pt 8):2107–15. [PubMed: 7983172]

Shaffer BM. Secretion of cyclic AMP induced by cyclic AMP in the cellular slime mould Dictyostelium discoideum. Nature. 1975; 255(5509):549–52. [PubMed: 167286]

Sharan K, Siddiqui JA, Swarnkar G, Chattopadhyay N. Role of calcium-sensing receptor in bone biology. Indian J Med Res. 2008; 127(3):274–86. [PubMed: 18497443]

Shelden E, Knecht DA. Dictyostelium cell shape generation requires myosin II. Cell Motil Cytoskeleton. 1996; 35(1):59–67. [PubMed: 8874966]

Shutt DC, Wessels D, Wagenknecht K, Chandrasekhar A, Hitt AL, Luna EJ, Soll DR. Ponticulin plays a role in the positional stabilization of pseudopods. J Cell Biol. 1995; 131(6 Pt 1):1495–506. [PubMed: 8522606]

Silver IA, Murrills RJ, Etherington DJ. Microelectrode studies on the acid microenvironment beneath adherent macrophages and osteoclasts. Exp Cell Res. 1988; 175(2):266–76. [PubMed: 3360056]

Soll DR. Timers in developing systems. Science. 1979; 203(4383):841–9. [PubMed: 419408]

Soll DR. A new method for examining the complexity and relationships of “timers” in developing systems. Dev Biol. 1983; 95(1):73–91. [PubMed: 6825933]

Soll, DR. Methods for manipulating and investigating developmental timing in *Dictyostelium discoideum*. In: Spudich, J., editor. Methods in Cell Biology. Vol. 28. Academic Press Inc.; 1987. p. 413-431.

Soll DR, Mitchell L, Kraft B, Alexander S, Finney R, Varnum-Finney B. Characterization of a timing mutant of Dictyostelium discoideum which exhibits “high frequency switching”. Dev Biol. 1987; 120(1):25–37. [PubMed: 3102295]

Soll DR. The use of computers in understanding how animal cells crawl. Int Rev Cytol. 1995; 163:43–104. [PubMed: 8522423]

Soll, DR.; Voss, E. Two and three dimensional computer systems for analyzing how cells crawl. In: Soll, D.; Wessels, D., editors. Motion Analysis of Living Cells. John Wiley Inc.; 1998. p. 25-52.

Soll DR. Computer-assisted three-dimensional reconstruction and motion analysis of living, crawling cells. Comput Med Imaging Graph. 1999; 23(1):3–14. [PubMed: 10091863]

Soll DR, Voss E, Johnson O, Wessels D. Three-dimensional reconstruction and motion analysis of living, crawling cells. Scanning. 2000; 22(4):249–57. [PubMed: 10958392]

Soll DR, Wessels D, Heid PJ, Zhang H. A contextual framework for characterizing motility and chemotaxis mutants in Dictyostelium discoideum. J Muscle Res Cell Motil. 2002; 23(7-8):659–72. [PubMed: 12952065]

Soll DR, Wessels D, Heid PJ, Voss E. Computer-assisted reconstruction and motion analysis of the three-dimensional cell. Scientific World Journal. 2003; 3:827–41. [PubMed: 14532423]

Soll, DR.; Voss, E.; Wessels, D.; Kuhl, S. Computer-assisted systems for dynamic 3D reconstruction and motion analysis of living cells. In: Shorte, S., editor. Cell Motility. Germany: Springer Verlag; 2007. p. 365-384.

Sonnemann J, Knoll G, Schlatterer C. cAMP-induced changes in the cytosolic free Ca++ concentration in Dictyostelium discoideum are light sensitive. Cell Calcium. 1997; 22(1):65–74. [PubMed: 9232353]

Stepanovic V, Wessels D, Daniels K, Loomis WF, Soll DR. Intracellular role of adenylyl cyclase in regulation of lateral pseudopod formation during Dictyostelium chemotaxis. Eukaryot Cell. 2005; 4(4):775–86. [PubMed: 15821137]

Stites J, Wessels D, Uhl A, Egelhoff T, Shutt D, Soll DR. Phosphorylation of the Dictyostelium myosin II heavy chain is necessary for maintaining cellular polarity and suppressing turning during chemotaxis. Cell Motil Cytoskel. 1998; 39:31–51.

Sugimoto T, Kanatani M, Kano J, Kaji H, Tsukamoto T, Yamaguchi T, Fukase M, Chihara K. Effects of high calcium concentration on the functions and interactions of osteoblastic cells and monocytes and on the formation of osteoclast-like cells. J Bone Miner Res. 1993; 8(12):1445–52. [PubMed: 8304045]

Sussman M. Cultivation and synchronous morphogenesis of Dictyostelium under controlled experimental conditions. Methods Cell Biol. 1987; 28:9–29. [PubMed: 3298997]

Taniura H, Sanada N, Kuramoto N, Yoneda Y. A Metabotropic Glutamate Receptor Family Gene in Dictyostelium discoideum. J Biol Chem. 2006; 218(18):12336–12343. [PubMed: 16527814]

Taylor CW. Controlling calcium entry. Cell. 2002; 111(6):767–9. [PubMed: 12526803]

Tomchik KJ, Devreotes PN. Adenosine 3′,5′-monophosphate waves in Dictyostelium discoideum: a demonstration by isotope dilution--fluorography. Science. 1981; 212(4493):443–6. [PubMed: 6259734]

Traynor D, Milne JL, Insall RH, Kay RR. Ca++ signalling is not required for chemotaxis in Dictyostelium. Embo J. 2000; 19(17):4846–54. [PubMed: 10970875]

Unterweger N, Schlatterer C. Introduction of calcium buffers into the cytosol of Dictyostelium discoideum amoebae alters cell morphology and inhibits chemotaxis. Cell Calcium. 1995; 17(2): 97–110. [PubMed: 7736566]

Varnum B, Soll DR. Effects of cAMP on single cell motility in Dictyostelium. J Cell Biol. 1984; 99(3):1151–5. [PubMed: 6088555]

Varnum B, Edwards KB, Soll DR. The developmental regulation of single-cell motility in Dictyostelium discoideum. Dev Biol. 1986; 113(1):218–27. [PubMed: 3943662]

Varnum-Finney BJ, Voss E, Soll DR. Frequency and orientation of pseudopod formation of Dictyostelium discoideum amebae chemotaxing in a spatial gradient: further evidence for a temporal mechanism. Cell Motil Cytoskeleton. 1987; 8(1):18–26. [PubMed: 2820592]

Veltman DM, Keizer-Gunnik I, Van Haastert PJ. Four key signaling pathways mediating chemotaxis in Dictyostelium discoideum. J Cell Biol. 2008; 180(4):747–53. [PubMed: 18299345]

Vicker MG, Grutsch JF. Dual chemotaxis signalling regulates Dictyostelium development: intercellular cyclic AMP pulses and intracellular F-actin disassembly waves induce each other. Eur J Cell Biol. 2008; 87(10):845–61. [PubMed: 18554748]

Wessels D, Soll DR, Knecht D, Loomis WF, De Lozanne A, Spudich J. Cell motility and chemotaxis in Dictyostelium amebae lacking myosin heavy chain. Dev Biol. 1988; 128:164–177. [PubMed: 2838348]

Wessels D, Schroeder NA, Voss E, Hall AL, Condeelis J, Soll DR. cAMP-mediated inhibition of intracellular particle movement and actin reorganization in Dictyostelium. J Cell Biol. 1989; 109(6 Pt 1):2841–51. [PubMed: 2556407]

Wessels D, Vawter-Hugart H, Murray J, Soll DR. Three-dimensional dynamics of pseudopod formation and the regulation of turning during the motility cycle of Dictyostelium. Cell Motil Cytoskeleton. 1994; 27(1):1–12. [PubMed: 8194106]

Wessels D, Voss E, Von Bergen N, Burns R, Stites J, Soll DR. A computer-assisted system for reconstructing and interpreting the dynamic three-dimensional relationships of the outer surface, nucleus and pseudopods of crawling cells. Cell Motil Cytoskeleton. 1998; 41(3):225–46. [PubMed: 9829777]

Wessels D, Zhang H, Reynolds J, Daniels K, Heid P, Lu S, Kuspa A, Shaulsky G, Loomis WF, Soll DR. The internal phosphodiesterase RegA is essential for the suppression of lateral pseudopods during Dictyostelium chemotaxis. Mol Biol Cell. 2000; 11(8):2803–20. [PubMed: 10930471]

Wessels D, Brincks R, Kuhl S, Stepanovic V, Daniels KJ, Weeks G, Lim CJ, Spiegelman G, Fuller D, Iranfar N, et al. RasC plays a role in transduction of temporal gradient information in the cyclic-AMP wave of Dictyostelium discoideum. Eukaryot Cell. 2004; 3(3):646–62. [PubMed: 15189986]

Wessels D, Kuhl S, Soll DR. Application of 2D and 3D DIAS to motion analysis of live cells in transmission and confocal microscopy imaging. Methods Mol Biol. 2006a; 346:261–79. [PubMed: 16957296]

Wessels D, Srikantha T, Yi S, Kuhl S, Aravind L, Soll DR. The Shwachman-Bodian-Diamond syndrome gene encodes an RNA-binding protein that localizes to the pseudopod of Dictyostelium amoebae during chemotaxis. J Cell Sci. 2006b; 119(Pt 2):370–9. [PubMed: 16410554]

Wessels D, Lusche D, Kuhl S, Heid P, Soll DR. PTEN plays a role in the suppression of lateral pseudopod formation during Dictyostelium motility and chemotaxis. J Cell Sci. 2007; 120(Pt 15): 2517–31. [PubMed: 17623773]

Wheeler GL, Brownlee C. Ca++ signaling in plants and green algae--changing channels. Trends Plant Sci. 2008; 13(9):506–14. [PubMed: 18703378]

Wick U, Malchow D, Gerisch G. Cyclic-AMP stimulated calcium influx into aggregating cells of Dictyostelium discoideum. Cell Biol Int Rep. 1978; 2(1):71–9. [PubMed: 204423]

Wokosin DL, Loughrey CM, Smith GL. Characterization of a range of fura dyes with two-photon excitation. Biophys J. 2004; 86(3):1726–38. [PubMed: 14990500]

Yamaguchi T, Chattopadhyay N, Kifor O, Butters RR Jr, Sugimoto T, Brown EM. Mouse osteoblastic cell line (MC3T3-E1) expresses extracellular calcium (Ca++o)-sensing receptor and its agonists stimulate chemotaxis and proliferation of MC3T3-E1 cells. J Bone Miner Res. 1998; 13(10): 1530–8. [PubMed: 9783541]

Yumura S, Furuya K, Takeuchi I. Intracellular free calcium responses during chemotaxis of Dictyostelium cells. J Cell Sci. 1996; 109(Pt 11):2673–8. [PubMed: 8937985]

Yumura S, Uyeda TQP. Myosins and cell dynamics in cellular slime molds. Int Rev Cytol. 2003; 224:173–225. [PubMed: 12722951]

Yumura S, Yoshida M, Betapudi V, Licate LS, Iwadate Y, Nagasaki A, Uyeda TQ, Egelhoff TT. Multiple myosin II heavy chain kinases: roles in filament assembly control and proper cytokinesis in Dictyostelium. Mol Biol Cell. 2005; 16(9):4256–66. [PubMed: 15987738]

Zhang H, Wessels D, Fey P, Daniels K, Chisholm RL, Soll DR. Phosphorylation of the myosin regulatory light chain plays a role in motility and polarity during Dictyostelium chemotaxis. J Cell Sci. 2002; 115(Pt 8):1733–47. [PubMed: 11950890]

Zhang H, Heid PJ, Wessels D, Daniels KJ, Pham T, Loomis WF, Soll DR. Constitutively active protein kinase A disrupts motility and chemotaxis in Dictyostelium discoideum. Eukaryot Cell. 2003; 2(1):62–75. [PubMed: 12582123]

Zheng JQ, Poo MM. Calcium signaling in neuronal motility. Annu Rev Cell Dev Biol. 2007; 23:375–404. [PubMed: 17944572]

Zigmond SH. Ability of polymorphonuclear leukocytes to orient in gradients of chemotactic factors. J Cell Biol. 1977; 75(2 Pt 1):606–16. [PubMed: 264125]

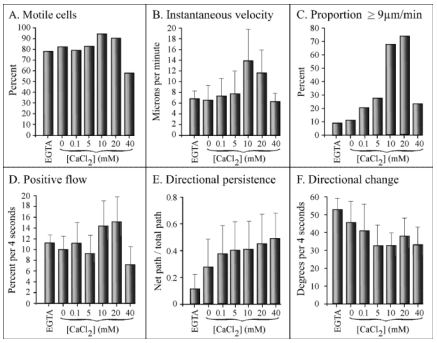

Figure 1.

Extracellular calcium regulates velocity and turning in the absence of chemoattractant. Cells were analyzed in a Sykes-Moore perfusion chamber. All test solutions were made in tricine buffer (TB) which contained 5 mM K^+, pH 7.0. Test solutions tested were tricine buffer plus 5 mM EGTA (EGTA), or tricine buffer containing 0 to 40 mM $CaCl_2$. Error bars represent the standard deviation of the means. At least 10 cells were analyzed in each of three independent experiments and the data pooled.

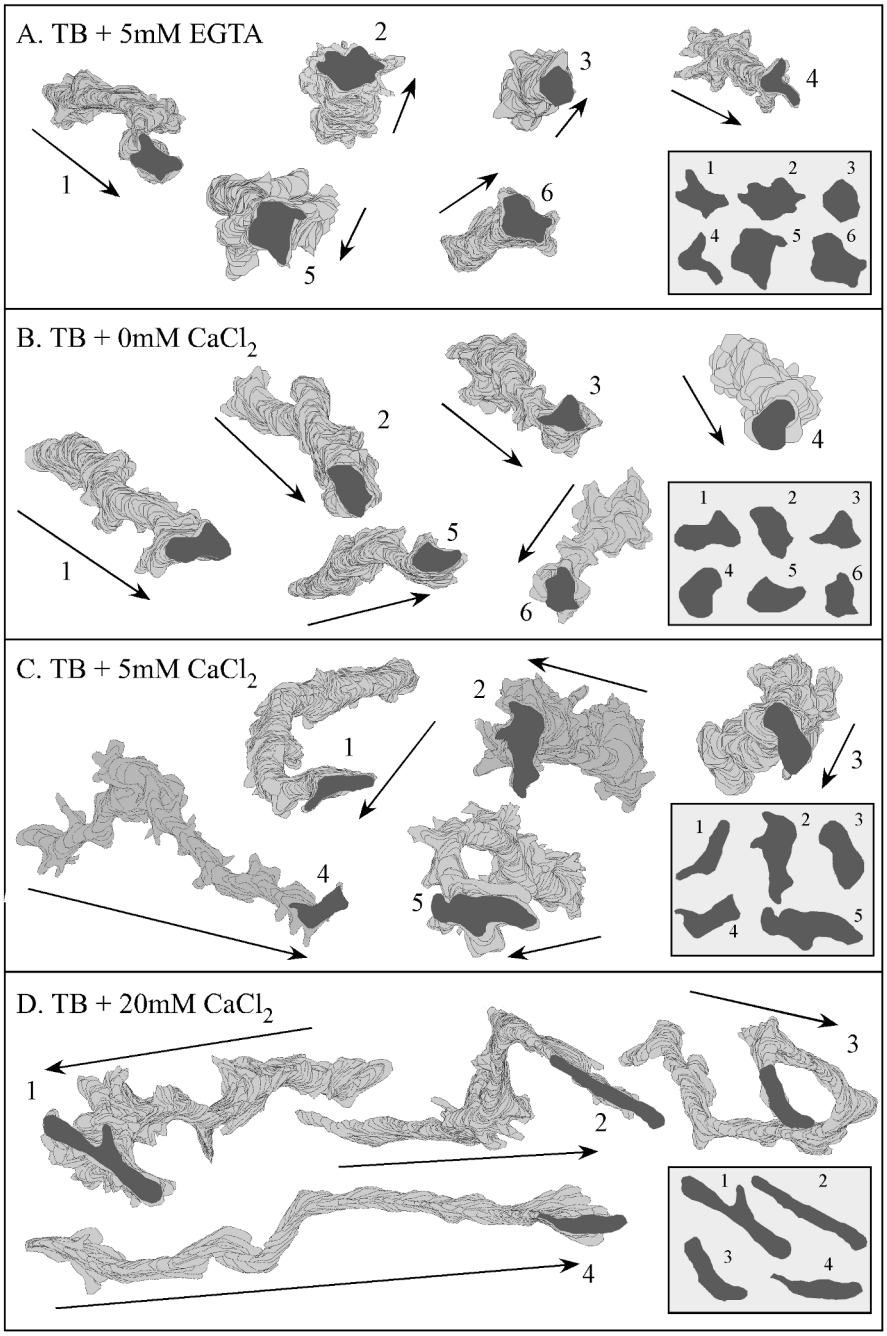

Figure 2.

Extracellular calcium regulates the length of perimeter tracks and cell shape in the absence of chemoattractant. See legend to Figure 1 for details. Cell perimeters were obtained at 4 sec intervals for 10 min and smoothed with Tukey windows (Soll, 1995). Outlines were drawn every 12 sec. Insets in the lower right of each panel show shapes at the end of the track for the representative cells. The numbers refer to the individual cells monitored. Arrows indicate average direction of transduction. TB, tricine buffer.

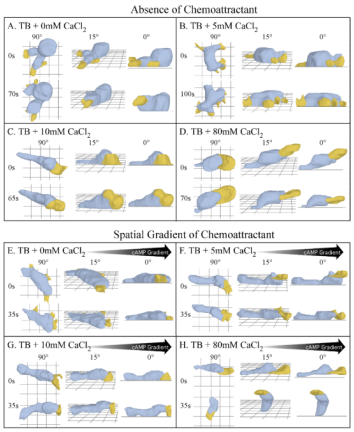

Figure 3.

3D reconstructions using 3D-DIAS software reveal that extracellular calcium regulates cell shape, pseudopod dynamics, uropod formation, adhesion to the substratum and uropod formation, in the absence of chemoattractant and in a gradient of cAMP gradient. A through D. Representative 3D reconstructions in test solutions in the absence of chemoattractant. E through H. Representative 3D reconstructions in test solutions in the presence of a spatial gradient of cAMP. In each case the cell is viewed at two time points and three different angles (90°, 15°, 0°). Blue represents cell body; yellow represents pseudopods; s, seconds. Black arrows represent the direction of the cAMP gradient in panels E through H.

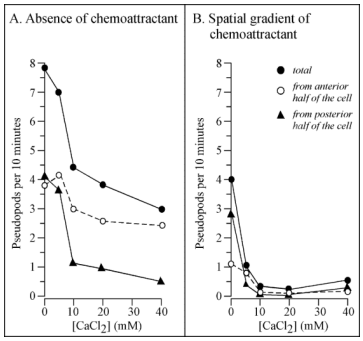

Figure 4.

Extracellular calcium regulates lateral pseudopod formation in the absence of cAMP (A) and in a spatial gradient of cAMP (B). Pseudopods were identified and counted as described in Methods section. The mean is presented for 10 cells at each concentration. The standard deviation was less than 50% of the mean for all data points ≥ 2.4, and no greater than the mean for all data points ≤ 1.3.

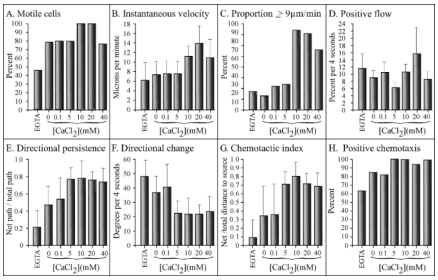

Figure 5.

Extracellular calcium regulates velocity, turning and the efficiency of chemotaxis in a spatial gradient of cAMP. Cells were analyzed in a spatial gradient chamber. See legend to Figure 1 for details of basic test solutions. Error bars represent the standard deviations of the means. At least ten cells were analyzed in each of three independent experiments and the data pooled.

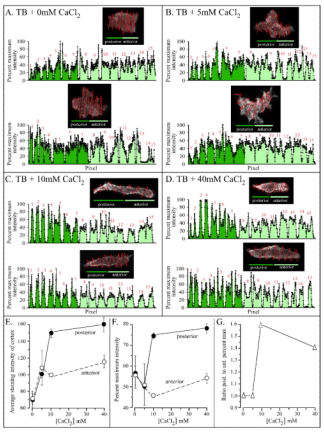

Figure 6.

Extracellular calcium regulates localization of myosin II in the cell cortex. Cells were stained with anti-myosin II antibody, and a confocal microscope projection image derived from the center five sections analyzed for pixel intensity through a zig-zag scan. The anterior and posterior ends of amorphous cells were identified by the location of tail probes (Heid *et al.*, 2005). Percent maximum intensity was computed from the most intense point (100%) in the scan. Data for the anterior half of the cell is dark green, and that for the posterior half light green. A through D. Scans for representative cells in test solution in the absence of cAMP. The zigzag track of the scan is presented in the dark box and the percent maximum intensity is plotted along the zigzag ("pixel") scan for each analyzed cell. E. Average staining intensities of the cortex of the anterior and posterior halves of five test cells as a function of $CaCl_2$ concentration in TB. F. Percent maximum intensities of the cortex of the anterior and posterior halves of five test cells as a function of $CaCl_2$ concentration in TB. G. Ratio of the percent maximum intensity of posterior to anterior half as a function of $CaCl_2$ concentration in TB. Error bars represent standard deviations of the means.

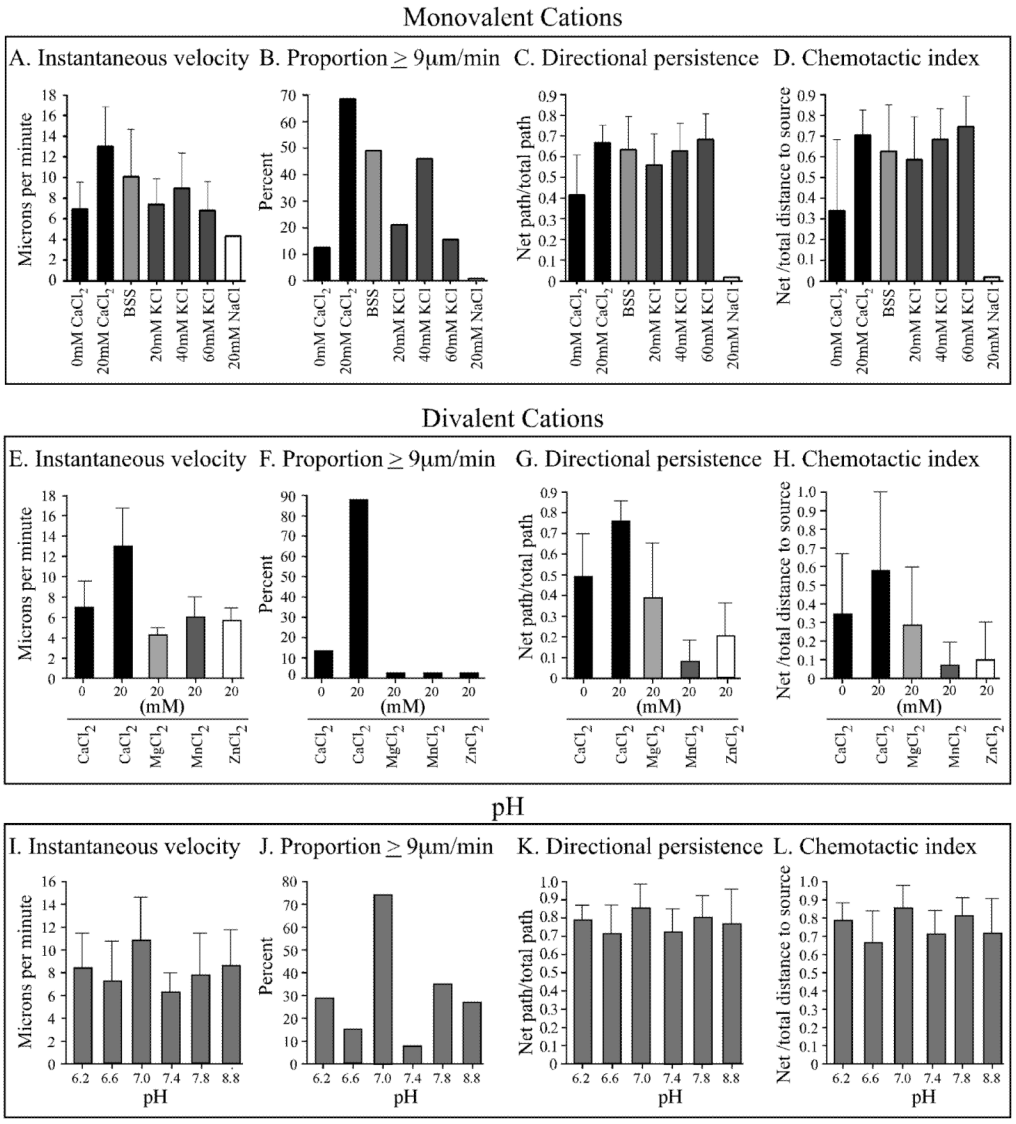

Figure 7.

Extracellular potassium substitutes for extracellular calcium in the presence of a spatial gradient of cAMP. A through D. A comparison of the effects of the buffered salt solution BSS, and TB containing 0 and 20 mM $CaCl_2$, 20, 40 and 60 mM KCl and 20 mM $NaCl_2$. The main cation in BSS is 40 mM K^+, it contains no added Ca^{++}. E through H. A comparison of the effects of divalent cations on behavior and chemotaxis. With the exception of BSS, all test solutions but BSS contained TB plus the noted concentration of each monovalent or divalent cation. I through L. Analysis of the effects of pH. pH was adjusted in TB buffer in the presence of 10 mM $CaCl_2$. Cells were analyzed in a spatial gradient of cAMP. Error bars represent standard deviations of the means.

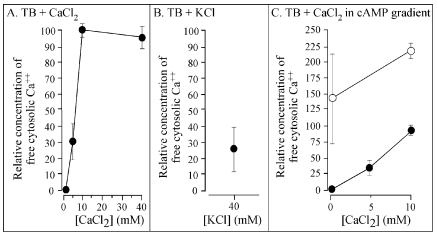

Figure 8.

Extracellular $CaCl_2$, KCl and a spatial gradient of cAMP induce increases in free cytosolic Ca^{++}. Cells were loaded with Fura-2-dextran then analyzed by fluorescent imaging methods in test solutions. All data points represent the mean of the relative free cytosolic Ca^{++} normalized to the highest data point obtained at 10 or 20 mM $CaCl_2$ in each of five independent experiments. The error bars represent the standard deviation of the means for the five experiments. A. Relative free cytosolic Ca^{++} in TB containing 0 to 40 mM $CaCl_2$. B. Relative free cytosolic Ca^{++} in TB containing 40 mM KCl. C. Relative free cytosolic Ca^{++} in a spatial gradient of cAMP (open circles), and in the absence of cAMP (closed circles) in 0 and 10 mM $CaCl_2$.

Table 1

The effects of a cAMP gradient and KCl on the localization of myosin II in the cortex of cells.

	No cAMP	cAMP gradient			cAMP gradient
	0 mM $CaCl_2$	**0 mM $CaCl_2$**	**5 mM $CaCl_2$**	**10 mM $CaCl_2$**	**.40 mM KCl**
Posterior staining intensity	61±11	178±20	193±31	202±26	192±29
Anterior staining intensity	64±14	166±5	145±31	118±8	158±23
Staining ratio, posterior to anterior	0.96±.015	1.09±0.12	1.40±0.30	1.70±0.21	1.30±0.13

Table 2

Comparison of the effects of extracellular $CaCl_2$, KCl and a spatial gradient of cAMP on behavior, cell morphology and myosin II localization.

Parameters[a]	0 mM $CaCl_2$ (no cAMP)	0 mM $CaCl_2$ (cAMP grad.)[b]	10 mM $CaCl_2$ (no cAMP)	10 mM $CaCl_2$ (cAMP grad.)[b]	40 mM K^+Cl_2 (no cAMP)
Inst. Velocity	6μm/min	7μm/min	14μm/min	14μm/min	9μm/min
Proportion ≥ 9μm/min	10%	15%	65%	92%	45%
Persistence	0.25	0.45	0.40	0.80	0.60
Dir. change	45 deg/4sec	35 deg/4sec	30 deg/4 sec	20 deg/4 sec	30 deg/4 sec
Uropod	no	no	yes	yes	yes
Rel. cort. myo II. ant.	70	165	100	120	160
Rel. cort. myo II. post.	70	175	150	200	190
Ratio cort. myo II (post/ant)	1.0	1.1	1.6	1.7	1.3
Ant. ps. form.	4/10 min	1/10 min	4/10 min	0.2/10 min	n.p.
Post. ps. form.	4/10 min	3/10 min	1/10 min	0.2/10 min	n.p.
Chem. index	n.a.	+0.3	n.a.	+0.8	+0.7
% pos chem.	n.a.	80%	n.a.	95%	90%

[a] Inst. velocity, instantaneous velocity; Dir. change, directional change; Rel. cort. myo II. ant. or post., relative cortical myosin II anterior or posterior, respectively; Ant. ps. form., anterior pseudopod formation; Post. ps. form., posterior pseudopod formation; Chem. index, chemotactic index; % pos. chem.., percent positive chemotaxis. Average values of parameters have been rounded off.

[b] cAMP grad., cAMP gradient.

[c] n.a., not available.

[d] n.p., not performed.